Low-temperature coupling of methane

CATAL. REV.—SCI. ENG., 38(2), 249–296 (1996)

Low-Temperature Coupling of Methane

LÁSZLÓ GUCZI,[1] RUTGER A. VAN SANTEN,[2] and K. V. SARMA[1]

[1]Department of Surface Chemistry and Catalysis
Institute of Isotopes of the Hungarian Academy of Sciences
PO Box 77, Budapest, Hungary, H-1525
[2]Schuit Institute of Catalysis
University of Technology Eindhoven
PO Box 513, 5600 MB Eindhoven, The Netherlands

I. INTRODUCTION

Methane is the main component of natural gas and its utilization amounts to ca. 1.7×10^9 tons of oil equivalent per year [1]. Since the present reserve of methane is located in remote places, its transportation is a major problem. Methane coupling to form C_{2+} hydrocarbons is, therefore, of a primary importance because before transportation methane should be converted into hydrocarbons with higher boiling points, such as ethane, propane, etc. The catalytic conversion of methane can be carried out in several ways which have excellently been reviewed in Refs. 1 and 2. Basically, three routes exist: (i) the indirect route in which methane is first converted into syngas in presence of water (steam reforming), CO_2 (carbon dioxide reforming), or oxygen (partial oxidation) and the resultant syngas can be utilized in the traditional way; (ii) direct coupling in the presence of oxygen (oxidative coupling of methane, OCM) or hydrogen (two-step polymerization); and (iii) direct conversion in the presence of oxygen to oxygenates (CH_3OH, HCOH), in the presence of Cl_2, HCl to methane chlorides, in the presence of ammonia to HCN, etc.

The most widely studied process is the OCM, which has been comprehensively surveyed by Baerns et al. [3], and OCM has been regarded as the most accepted route. Results of the research carried out so far have shown that the best catalyst is Li/MgO with or without promotion. Here, in the presence of oxygen, methyl radicals are formed which may recombine in the gas phase, and this results in the formation of higher hydrocarbons. Pasquon [4] has reported the best result obtained in long-run tests, namely, 15% C_{2+} yield versus methane with 15–40% conversion and 75–40% respective selectivity at 1270–1370 K and at 1–2 bar pressure using a 5–10 CH_4/O_2 ratio. Further details about this process have been summarized by Lunsford [5] and Fierro [6].

Indirect methane conversion, in which natural gas is first converted to syngas at high temperature [7], produces subsequently hydrocarbons in a low-temperature exothermic process from syngas, either by Fischer–Tropsch synthesis [8,9], by the methanol to gasoline (MTG) process via methanol [10], or by Shell Middle Distillate Synthesis [11].

Direct methane conversion, like pyrolysis to acetylene and benzene [12], operates only at temperature above 1200 K [13].

Oxidative coupling of methane to ethylene has been proposed as a promising alternative route [13–19]. This reaction results in C_{2+} hydrocarbon yields up to 25% when the reaction is performed at temperatures around 1100 K. To increase the catalyst life and the selectivity for C_{2+} hydrocarbons, processes operating at low temperatures are becoming more importance [20,21]. However, in 1994 Jiang et al. [22] discovered an improved method in which again a high-temperature (1270 K) gas recycle is utilized in an electrocatalytic or catalytic reactor with a loop where ethylene is effectively retained in a molecular sieve trap and the C_2 hydrocarbon yield amounts to 88% despite the fact that electrochemical conversion was estimated to be the most costly process [23].

In the recent progress on OCM, "oxidation to syngas" based processes have achieved considerable improvement. Partially reducible oxides, such as MnO_2, K-promoted Mn_3O_4, perovskites, etc., were applied to supply oxygen for the removal of the first hydrogen atom from methane, and in a separate step the catalyst was reoxidized (see, e.g., Refs. 1, 24, and 25). Despite these improvements, Rostrup-Nielsen [2] claims that in syngas-based routes ca. 20% of carbon in the feed was converted into CO_2. Consequently, the metal-catalyzed transformation of CH_4 into a reactive surface CH_x species and the subsequent combinations of CH_x species in presence of hydrogen to produce higher molecular weight hydrocarbons could be a feasible alternative route to oxidative coupling.

During the last 6 years several excellent reports were published which showed the importance of methane coupling [26].

In the present review we focus on methane coupling under oxygen-free conditions. Within this subject (i) activation of C–H bond (primarily in methane) and (ii) C–C bond formation between CH_x fragments and between those and some higher hydrocarbon fragments are considered particularly, which could have relevance to the mechanism of higher hydrocarbon formation.

First, theoretical studies on CH_4 adsorption are considered following the interaction of methane with metal surface. Then we discuss the formation, structure, and role of surface carbonaceous species; and then the surface science approach of C–H bond rupture on metal surfaces is reported. The major part of this article is the mechanism of the nonoxidative methane coupling, including the relevance of the surface carbon species, the two-step reaction to form hydrocarbons low-temperature homogeneous methane activation, the use of membrane catalysts, etc. We briefly discuss the possible roles of promoters and alloys in the reaction of C_n building processes.

Direct and indirect oxidation of methane with participation of dioxygen (in presence or absence of ammonia, chlorine compounds, etc.) are outside the scope of this review.

II. THEORETICAL STUDIES OF ADSORBED CH_x SPECIES

The feasibility of the various elementary reactants including methane is expressed by the difference in standard free energies at various temperatures. The energies of the homolytic or heterolytic dissociation of methane (and several higher hydrocarbons) are also characteristic of the methane reactivities. The respective values are presented in Tables 1 and 2 [27,28]. Generally speaking, reactions with large negative free energy changes (e.g., combustion; not indicated in Table 1) resulted in products with low price values, while those with positive free energy changes led to valuable products. Anyhow,

TABLE 1

Thermodynamic Data, Change of Free Energy, $\Delta G°$, for Methane Transformation [28]

Reactions	$\Delta G°$ (kcal mol^{-1})			
	400 K	600 K	800 K	1000 K
$2CH_4 \rightarrow C_2H_4 + 2H_2$	18.9	15.9	12.8	9.5
$2CH_4 \rightarrow C_2H_6 + H_2$	8.6	8.4	8.5	8.5
$2CH_4 + O_2 \rightarrow C_2H_4 + 2H_2O$	−34.6	−35.1	−35.8	−36.4
$2CH_4 + O_2 \rightarrow C_2H_6 + H_2O$	−18.4	−17.1	−15.8	−14.5
$CH_4 + O_2 \rightarrow CH_3OH$	−25.4	−23.0	−20.5	−18.0
$CH_4 + O_2 \rightarrow HCHO + H_2O$	−69.0	−70.0	−70.8	−71.2
$CH_4 + CO \rightarrow CH_3CHO$	16.0	21.9	27.7	33.6
$CH_4 + CO_2 \rightarrow CH_3COOH$	19.2	24.9	30.4	35.5
$CH_4 + H_2O \rightarrow CO + 3H_2$	28.6	17.3	5.5	−6.5
$CH_4 + C_2H_4 \rightarrow C_3H_8$ ($\Delta G°$ at 300 K = −6.2)	−6.4	0.1	6.5	12.8

TABLE 2

Dissociation Energy, ΔH_d, Values for C–H Bond Dissociation [29]

Dissociation mechanism	ΔH_d (kJ mol^{-1})
Homolytic cleavage	
$CH_4 \rightarrow CH_3 + H$	435
$C_2H_6 \rightarrow C_2H_5 + H$	410
Heterolytic cleavage	
$CH_4 \rightarrow CH_3^- + H^+$	1690
$C_2H_4 \rightarrow C_2H_3^- + H^+$	1690
$C_3H_6 \rightarrow C_3H_5^- + H^+$	1640
$C_2H_2 \rightarrow C_2H^- H^+$	1580

the primary process in all cases, regardless of the thermodynamics, was the dissociation of methane to CH_x species which was associated with their coupling on the surface.

Van Santen et al. [29] theoretically studied the reaction path for recombination of surface CH_x species on Rh_{40} and Pd_{40} clusters simulating a *fcc*(111) surface, using the semiempirical atom superposition and electron delocalization (ASED) method. Highly hydrogenated surface carbon fragments are found to have high activation energies for recombination due to steric hindrance by the hydrogen atoms. The lowest activation energy was found for the recombination of threefold-bonded carbon atoms with a CH_2 species to form a vinylidene intermediate. By comparing this reaction step on clusters simulating ruthenium and palladium clusters, it appeared that the activation energy for C–C bond formation is rather insensitive to metal–carbon bond strength. The results obtained on silica-supported Rh, Co, and Ru catalysts confirm that C–C bond formation is favorable from CH_x fragments in which the average value of x is 1.

Yang et al. [30] described the chemisorption of atomic hydrogen and C_1 fragments (CH, CH_2, and CH_3) on Ni(111) surface. The main features can be summarized as follows:

- Dissociated H, CH, CH_2, and CH_3 species are bonded strongly to the Ni(111) surface at the threefold and bridge sites. The relative bond strengths are CH > CH_2 > H > CH_3, with corresponding maximum adsorption energies of 3.1, 2.9, 2.7, and 1.7 eV. The atop–atom adsorption sites are energetically rather unfavorable for H, CH, and CH_2, and are 0.2 eV higher in energy for CH_3 than adsorption at threefold sites. Except for the atop site, the Ni(111) potential surface appears fairly flat for H and CH_x fragments.
- The calculated bond distances at the bridge and threefold sites are 0.181 and 0.187 nm for Ni—H, 0.2 and 0.204 nm for Ni—C in CH and CH_2, and 0.233 and 0.235 nm for Ni—C of CH_3 species.
- Vibrational frequencies for the surface adsorbate species are 1043 to 1183 cm^{-1} for M—H, 450 to 600 cm^{-1} for M—C in CH, 430 to 500 cm^{-1} for M—C in CH_2, and 296 to 416 cm^{-1} for M—C in CH_3 at the different adsorption sites. The C—H stretching frequencies for CH, CH_2, and CH_3 are around 3000 cm^{-1} for adsorption in their equilibrium geometry.
- A low C—H vibrational frequency of methyl group on the Ni(111) is calculated at 2627 cm^{-1} is one of the hydrogens is tilted parallel to the surface, and CH_3 is shifted away from the threefold center by 0.67 a.u. This geometry is only 0.07 eV higher than the calculated equilibrium geometry.
- Calculated equilibrium geometries are as follows: CH is perpendicular to the surface, CH_2 lies in a plane inclined by about 293° to the

surface normal with a symmetric orientation of hydrogens. For CH_3 species by the hydrogens are in a plane parallel to the surface with a nearly tetrahedral configuration. Threefold adsorption sites are the most stable positions for all adsorbates, but bridge sites have comparable stability (0.1 to 0.2 eV higher in energy).

- The reactions of $CH_{(ads)} + H_{(ads)}$ electron transfer from the surface to each adsorbate was accompanied by a work function increase of about 0.1 to 0.2 eV.

The relation between stronger adsorbed carbon atoms and the C—C coupling reaction was also studied with theoretical calculations using the ASED molecular orbital theory based on an extended Hückel calculation [31]. The metal–carbon bond strength decreased in the order Ru > Rh > Pd, whereas the activation energy for C–C bond formation is hardly changed. The adsorption energies (in electron volts) for CH_x fragments on Ru, Rh, and Pd *fcc*(111) metal cluster of 40 atoms as calculated by ASED are presented in Table 3.

Calculations using the linear combination of atomic orbitals (LCAO) method [32] indicate that carbon is bonded more strongly on Ru than on Rh and Pd. Experimentally it was found [33] that the selectivity for C_{2+} hydrocarbons in the syngas reaction decreased from Ru to Pd. So, for good C_{2+} hydrocarbon selectivity the interaction between the adsorbed CH_x fragments and the metal surface has to be high. However, if the interaction of carbon atoms with the metal surface becomes very strong (e.g., tungsten), stable carbides can be formed which can lead to a strongly diminished catalytic activity.

Recently, van Santen [34] studied the reactivity of transition metal surfaces and concluded that adsorbed atoms usually favored high coordination sites. Their adsorption energy decreases strongly with an increased d-valence electron occupation, due to the occupation in the antibonding adsorbate-surface fragment orbitals. The adsorption energy of a molecule is controlled by the balance between the donating (HOMO) and backdonating (LUMO) interaction terms. Backdonation favored high, while donation favours low coordination. The interaction with the d-valence electrons controls the balance.

TABLE 3

Adsorption Energies (eV) of CH_x Species [31]

Species	Ru	Rh	Pd
CH_3	−2.70	−2.58	−2.2
CH_2	−4.07	−3.77	−2.93
CH	−5.64	−5.45	−4.46
C	−5.51	−5.47	−4.47

Bond order conservation predictions agree qualitatively with the dependence of surface atom reactivity on the surface metal atom coordination. It leads to a decreased surface atom reactivity with increasing surface electron delocalization. Bond order conservation principles are not always useful for predictions of surface coordination of molecules, because of the balance between the different interaction terms that often controls the chemical bond strength of the adsorbed molecules.

Joyner [35] summarized that the slow step in chain growth during Fischer-Tropsch (FT) synthesis is the formation of an adsorbed ethylidene species from two adsorbed methylenes. Addition of a further methylene species gives diadsorbed C_3H_6 entities, which leads to a singly attached carbonium ion. A 1,2-hydrogen shift then forms a methyl-substituted ethylidene species, which is available for further polymerization. Further hydrogen shift may occur, yielding olefin molecules and terminating the chain growth.

Using the bond order conservation Morse potential (BOC-MP) approach applied by Shustorovich [36], the effects of metal on FT synthesis was studied by calculating the energetics of the conceivable elementary steps during CO hydrogenation over the periodic series of Fe(110), Ni(111), Pt(111), Cu(111). It was shown that the periodic trends in the ability of metal surfaces to dissociate chemical bonds and those to recombine the bonds were always opposite; particularly, metallic Fe was necessary to produce an abundance of carbidic carbon from CO. However, synthesis of the hydrocarbons and oxygenates effectively proceeded only on carbided Fe surfaces which resembled the less active metals such as Pt. More specifically, the C—C chain growth should occur predominantly via CH_2 insertion into the metal–alkyl bond and the primary FT products should have been α-olefins.

The bonding of CH_3, CH_2, and CH fragments to Ti(0001), Cr(110), and Co(0001) metal surfaces was examined by Hoffmann et al. [37] with extended Hückel band calculations on two-dimensional slabs of metal and adsorbate. All CH_x fragments tend to restore their missing C–H bonds when bound to these surfaces: CH_3 prefers the atop site, CH_2 the bridging, and CH the capping geometry. CH_3 species are anchored more strongly to the atop site of the metal surface of higher d-band filling since the antibonding feature at the atop of the d-band destabilized sites are of higher coordination. Similar conclusions were applied for other fragments. Thus, the mobility of these fragments is reduced on metal surfaces of higher d-band filling. When two C_1 fragments are coupled, the C—C σ^* orbital rises from below the Fermi level. It is initially filled and then empties as the reaction proceeded. Hence, the lower the Fermi level, the smaller the reaction barrier is.

In conclusion, theoretical studies emphasize two factors controlling the fate of CH_x on the surface. Primarily, the nature of the metal controls the strength of metal–carbon bonds, ranging from high (carbide formation) to weak (partially hydrogen containing species) bond strength. Secondly, surface morphology affects and further modifies the reactivity of the CH_x ($0 < x < 3$) species.

III. INTERACTION OF METHANE WITH METAL SURFACES

Methane is the most stable molecule among hydrocarbons; it is, therefore, difficult to activate. Its activation can be facilitated by pressure, as Beckerle et al. reported [38]. They proposed a mechanism called "chemistry with a hammer," in which the methane molecules adsorbed at low temperature were activated by collisions with other particles. In this section, however, we wish to deal with chemical and catalytic activations of methane, particularly with the activation of methane chemisorbed over metal surfaces. Interactions between metals and simple hydrocarbons have been exhaustively discussed earlier [39]; thus, here only those results are presented which are closely related to methane coupling.

Methane decomposition takes place most effectively on small nickel particles, as studied by Kuijpers et al. [40,41]. They studied the interaction of methane with a silica-supported nickel catalyst at temperatures between 303 and 620 K, in both continuous-flow and pulse-flow experiments [40]. The activation energy for chemisorption was estimated to be at 6 kcal mol^{-1}. At temperatures above 448 K, the methane adsorbed over nickel and dissociated completely into adsorbed carbon atoms and hydrogen. The hydrogen released shifts the equilibrium

$$CH_{4(g)} \leftrightarrow C_{(ads)} + 4H_{(ads)}$$

to the left side. Reactivity of the carbonaceous species deposited appeared to be small at 373 K, but at 473 K these species were the most reactive toward hydrogen. When—after a number of hydrogen pulses—the temperature of the catalyst was further raised to 573 K in nitrogen flow, a considerable amount of methane was evolved.

The low-field magnetic method and infrared spectroscopy were also applied to measure the adsorption of methane on silica-supported nickel catalysts at various constant temperatures (303 K < T < 373 K) and at increasing temperatures (303 K < T < 573 K) by Kuijpers et al. [41]. In the entire temperature range the chemisorbed methane was found to dissociate according to the reaction

$$CH_4 + 7Ni \rightarrow Ni_3C \text{ ("surface nickel-carbide")} + 4Ni—H$$

It was observed that, per unit surface area, small nickel crystallites were more reactive toward methane than larger ones.

Kuijpers et al. [42] also studied the chemisorption of hydrogen on both bare and carburized Ni/SiO_2 catalysts by means of the low-field magnetic method Fourier-transform infrared spectroscopy (FTIR), and mass spectrometry. The less steep slope of the magnetization-volume isotherm at elevated temperatures was ascribed to a more extensive coverage of smaller nickel particles after admission of the initial H_2 doses.

Carburization of the catalysts was established by the decomposition of

methane at temperatures from 303 to 573 K. At low surface coverages the carbon was deposited as Ni_3C, strongly affecting magnetization. At higher surface coverages, CH_x complexes were chemisorbed without any effect on the magnetization. After decomposition of methane, the nickel samples were evacuated at 623 K resulting in the conversion of a part of the carbonaceous deposits into methane. Also, with subsequent chemisorption of hydrogen on the carburized catalysts (T = 303 K), the reaction between chemisorbed hydrogen atoms and deposited carbon was indicated by the production of methane. From a comparison between the magnetization-volume isotherms measured for the H_2 chemisorption before and after deposition of small amounts of carbon, it was concluded that decomposition of methane proceeds preferentially on small nickel crystallites [41]. Finally, it was found that hydrogen was adsorbed not only on bare nickel (with a magnetic effect) but also on nickel carbide (without magnetic effect).

Erkelens and Wosten [43] studied methane adsorption on a Ni/SiO_2 catalyst using the low-field magnetic method and infrared (IR) measurements. Comparing the initial slopes of the methane and hydrogen isotherms, both measured at 298 K, they calculated that four to five surface bonds were formed by each methane molecule chemisorbed.

In early work of Gajdaj et al. [44], methane was adsorbed in the temperature range between 300 and 443 K over unsupported Ni samples. Between 45 and 200 torr of methane pressures the surface coverage changed between 0% and 85%. The adsorption kinetics obeyed the Roginskij–Zeldovits equation based on the assumption that the nickel surface is heterogeneous. The dissociation of methane at low temperature proceeds to CH_2 and the activation energy was 7 kcal/mol, which agreed with other data.

The activation energy obtained from measurement of methane adsorption over various Ni samples lies in the region of 7–9.6 kcal/mol, which is in agreement with the theoretical value calculated for Ni(100) using ab initio complete active space level contracted configuration interaction (CASSCF-CCI). Here, a cluster model was assumed with one active Ni atom at all-electron level, and 12 bulk atoms described by one-electron effective core potential [45].

On a number of VIIIB metals (Ru, Co, Ni), decomposition of methane proceeds with the formation of carbon, the characterization of which is essential to learn more about its reactivity in further reaction. On Ru α- and β-carbons were identified by solid-state nuclear magnetic resonance (NMR) and reported by Duncan et al. [46]. They suggested that α-carbon consists of isolated carbon atoms bonded to Ru atoms either on or below the surface of the metal crystallites. The NMR peak for β-carbon was originally ascribed to the carbon bonded to silicon atoms of the support. However, more recent work by these authors indicates that the β-carbon peak was better assigned to a combination of alkyl groups and highly mobile nonhydrogenated species. These studies also revealed the presence of a small amount of graphite like carbon [47].

Van Santen et al. [29] also assumed three types of (α-carbon, β-carbon and γ-carbon) surface carbonaceous species on ruthenium, the presence of which was earlier identified with NMR [47] and atomic emission spectroscopy (AES) [48,49]. Distinction between α-, β-, and γ-carbonaceous species could be made by hydrogenation at temperatures 323 K, 383–573 K, and >673 K, respectively, but these species can be in dynamic equilibrium [47,50]. The α-carbon species has been studied previously when generated from CO [51,52] and is responsible for higher hydrocarbon formation [53,54]. The optimum temperature for the formation of C_{2+} hydrocarbons depends on both the selectivity and the amount of surface carbonaceous intermediates hydrogenated. The optimum is around 378 K for Ru and Co catalysts. The maximum yield of 13% is obtained at a carbon surface coverage of 18%. The yield obtained on alumina (Ketjen, CK-300) was a little higher than those obtained on silica.

As was shown in the preceding paragraphs, on nonnoble transition metals (Ni, Co, and Fe) the carbon species are strongly bonded to the surface. Their reactivity, therefore, is very low. This is why noble transition metals, on which this interaction is weaker, have been the subject of several investigations.

Trevor et al. [55] studied methane decomposition on platinum metal clusters of different sizes and concluded that the methane decomposition rate was the highest for clusters of platinum dimer through to platinum pentamer (Pt_2–Pt_5).

Ponec et al. [56] estimated the reactivity of methane, ethane, and carbon monoxide on polycrystalline platinum and rhodium surfaces toward hydrogen using AES. They concluded that on Pt and Rh amorphous and graphitic carbon layers were produced from CO, CH_4, and C_2H_4. The rate of their formation on Pt with the various gases was $C_2H_4 > CH_4 > CO$. On Pt as well as on Rh some of this amorphous and graphitic-type carbon could be removed by hydrogen. The presence of hydrogen slows down the formation of this amorphous and graphitic carbon on both metals. The reactive amorphous and graphitic carbon layers are preserved on Rh to a greater extent than on Pt under comparable conditions.

Lisowski et al. [57] reported that methane is adsorbed on platinum thin films at 195 and 298 K in two distinct forms. The first type is formed with the increase in the surface potential and is stable during the isothermal evacuation of the system, while the second one, being adsorbed without a measurable change in the surface potential, is weakly bound and can be removed by isothermal evacuation of the system. Adsorption of the strongly bound form is an activated process: the number of molecules adsorbed in this form increases with increasing temperature from 195 to 298 K.

Brass et al. [58] concluded that excitation of internal motions, rather than translation, determines the rate of methane chemisorption on the rhodium surfaces.

Solymosi et al. [59] concluded that the silica-supported Pt metals were

found to be active in the decomposition of methane above 473 K to give hydrogen, a small amount of ethane, and different carbon species. Regarding the dissociation of methane, the most active metal was the Rh; the largest amount of ethane and higher hydrocarbons was measured on Pt/SiO_2, as shown in Table 4.

The reactivity of methane in the presence of CO_2 to yield CO and H_2 occurred above 700 K was different [60]. The specific activities of the Pt metals in terms of turnover frequencies decreased in the order Ru > Pd > Rh > Pt > Ir, as shown in Table 5. It was assumed that the activity order corresponds to the ability of Pt metals to dissociate CO_2 and to produce adsorbed oxygen atoms which scavenge hydrogen atoms from methane.

Further studies have been carried out on the dissociation of CH_4 and CO_2, as well as the reaction between these two molecules [61]. Over silica-

TABLE 4

Distribution of Hydrocarbons Formed During Hydrogenation of Surface Carbon Following Exposure of the Supported Noble Metals to Methane[a] [59]

	Products[b] (%)					
Catalyst	C_2H_6	C_3H_8	n-C_4H_{10}	i-C_4H_{10}	C_5	C_6
$5\%Ru/SiO_2$	1.16	0.65	—	—	—	—
$5\%Rh/SiO_2$	0.14	0.03	—	—	—	—
$5\%Pd/SiO_2$	—	—	—	—	—	
$5\%Pt/SiO_2$	42.9	10.4	2.2	0.8	7.8	2.7
$5\%Ir/SiO_2$	1.2	<0.1	0.2	—	—	—

[a]Conditions: catalyst 0.1 g; step 1, 1 min exposure of the catalysts to methane flow (200 mL/min) at 523K; step 2, the samples were treated with hydrogen pulses at 523 K.
[b]Other product was methane.

TABLE 5

Codecomposition of CH_4 and CO_2 on Supported Pt Metals at 773 K [60]

		CH_4 pulses		CO_2 pulses	
Catalyst	Dispersion (%)	CH_4 reacted (μmol)	C_2H_6 formed (μmol)	Carbon surface (μmol)	CO formed (μmol)
1% Ru	5.5	19.55	9.53	0.49	0.28
1%Rh	46.2	17.28	7.66	1.96	0.78
1%Pd	23.2	19.90	9.95	—	0.20
1%Ir	75.5	10.55	3.8	2.95	0.09
1%Pt	41.3	7.23	2.72	1.79	0.1

Note. The data are the total amount of the values obtained in 10 CH_4 and 10 CO_2 pulses. The amount of catalyst was 0.3 g; 1 pulse contained 32.6 μmol CH_4 or CO_2.

and alumina-supported rhodium in a fixed-bed continuous-flow reactor, the decomposition of methane on rhodium occurred above 423 K, resulting in the transient evolution of hydrogen and ethane. The rates of decomposition of methane and product distribution are influenced by the nature of the support. The most effective catalyst for hydrogen formation was Rh/Al_2O_3, which was followed by Rh/TiO_2, Rh/SiO_2, and Rh/MgO, but the highest ethane formation was observed on Rh/SiO_2. The large excess of hydrogen produced by the interaction of methane with supported Rh indicated the partial or full decomposition of methane to CH_x or surface carbon.

In order to identify the surface species formed, these researchers [61] performed detailed IR measurements, but they were unable to detect the transient species in methane dissociation. The reactive α-carbon species produced at 423–523 K was hydrogenated to methane even below 350–400 K. The majority of the surface carbon (β-form) reacted at 400–550 K, and the most unreactive γ-form reacted above 550 K. The distributions of these carbon forms and of the hydrogenation products were largely influenced by the length of time which the carbon was kept at 523 K. At low contact time (1 min) with methane at 523 K, higher hydrocarbons were also produced in addition to methane on Rh/SiO_2 (0.15% C_2H_6 and 0.03% C_3H_8). When the exposure time was extended to 10 min, only methane was evolved. The highly reactive α-form was missing, when the Rh samples were exposed to methane at higher temperatures (673–773 K.) Addition of methane to CO_2 promotes the dissociation of CO_2. Supported Rh is active in the high-temperature reaction of $CO_2 + CH_4$ to give hydrogen and carbon monoxide without carbon deposition.

Recent experiments demonstrate that hydrocarbon formation is possible at low temperature, once methane is activated. Shelimov and Kazansky [62] activated methane on a molybdenum oxide catalyst by photochemisorption at pressures between 50 and 6000 Pa. At room temperature upon desorption in vacuum ethene, ethane and propane were detected.

From the preceding experimental result it can be concluded that methane can be activated by VIIIB metals at moderate temperature. At higher temperature various forms of carbon are produced on the metal surface and only a part of these can be hydrogenated. Obviously, in coadsorption, methane proved to be the least active molecule.

IV. SURFACE SCIENCE APPROACH TO METHANE COUPLING

In order to have deeper insight into the mechanism of methane coupling as well as better understanding about the structure and composition of CH_x species, surface science studies should be reviewed.

The chemisorption and reaction of hydrogen and hydrocarbon fragments on catalytically active transition metal surfaces received a great deal of attention due to the commercial importance of hydrocarbon formation. Kamin-

sky et al. [63] first observed CH, CH_2, and CH_3 fragments on Ni(111) by secondary ion mass spectrometry (SIMS). X-ray photoelectron spectroscopy (XPS) and SIMS data suggested that the C_1 fragments have similar stabilities on Ni(111).

Schouten et al. [64,65], working with single crystals, established that the interaction of methane with metal a surface is strongly affected by the atomic structure of the surface. At 373 K the carbon content on a Ni(110) surface increased rapidly with exposure to methane, while that on the Ni(100) surface rose more slowly. On the other hand, the Ni(111) surface did not show measurable reaction with methane even at a more elevated temperature. Experiments with supported catalysts and vapor-deposited films indicated that at small hydrogen coverages, methane chemisorbs dissociatively on nickel surfaces. Hydrogen from the dissociation of carbon–hydrogen bonds is either chemisorbed or it desorbs as molecular hydrogen, depending on the temperature.

Beebe et al. [66] and Yates et al. [67] measured the sticking coefficient and activation energies for the activated dissociative adsorption of methane on nickel single-crystal surfaces. From these results the most likely elementary steps on Ni(111) seem to be the following:

$$C_{(ads)} + H_{(ads)} \rightarrow CH_{(ads)}$$
$$CH_{(ads)} + H_{(ads)} \rightarrow CH_{2(ads)}$$
$$CH_{2(ads)} + H_{(ads)} \rightarrow CH_{3(ads)}$$
$$CH_{3(ads)} + H_{(ads)} \rightarrow CH_{4(g)}$$

Their kinetic studies, using temperature-programmed desorption (TPD), suggested that the rate-determining step must be one of the successive decompositions that occurs at a stage prior to the $CH_{3(ads)} + H_{(ads)} \rightarrow CH_{4(g)}$.

Yang et al. [68] decomposed preadsorbed methane on a Ni(111) single-crystal surface by a krypton bombardment at 47 K under ultrahigh vacuum (UHV) conditions (5×10^{-8} Pa). The collision of the incident Kr with the physisorbed methane distorts first the tetrahedral configuration of methane, thereby lowering the barrier for the dissociation into adsorbed methyl radicals and an adsorbed hydrogen atom. At 230 K, all the adsorbed CH_3 surface species dissociates to adsorbed CH, and two CH can recombine to form adsorbed C_2H_2. Some of the C_2H_2 species are trimerized to adsorbed C_6H_6. The key to benzene formation is: (i) high C_2H_2 coverage on surface, (ii) removal of hydrogen from the surface.

The CH_x species formed on Ni(100) by hydrogenation of carbidic carbon were detected using high-resolution electron energy loss spectroscopy (HREELS) [69]. Exposures of carbidic carbon to 1×10^{-9} Pa H_2 and D_2 at 313 K for 20 min produce CH_x and CD_x species, respectively. These species are identified by two energy-loss peaks for CH_x at 2970 and 1380 cm^{-1}, and only one peak for CD_x at 1980 cm^{-1}. Due to the existence of the intense peak at 1380 cm^{-1}, which is assigned to the range of a scissor mode of CH_2

vibration and a symmetric deformation mode for CH_3, the CH_x species are tentatively ascribed to CH_2 and/or CH_3. The CD_x species undergo decomposition at 330–370 K in UHV as well as in hydrogen below 10^{-9} Pa. No stable CH_x species are observed above 400 K, which is lower than the normal reaction temperature for methanation reaction (500 K).

Ceyer and coworkers [70–72] studied the dynamics of the dissociative chemisorption of CH_4 on Ni(111) activated in molecular beam techniques using HREELS. A barrier to dissociative chemisorption of methane was found and products of the dissociation were identified by electron energy loss spectroscopy (EELS) as adsorbed CH_3 and H.

Hamza and Madix [73] have studied the dissociative chemisorption of saturated C_1–C_4 hydrocarbons on Ni(100) using supersonic molecular beam techniques. The translational activation, the initial sticking probability, the scattering distribution, and the adsorption kinetics were investigated. Rosei et al. [74,75] obtained quantitative values for activation energies and preexponential factors for dissociation of CH, CCH, and C_2H_2 species on Ni(111) surface by HREELS. Ni single crystals seem, therefore, to be an active surface toward the formation of strongly bonded carbon species and for hydrogenation at higher temperature to yield hydrocarbons.

McBreen et al. [76] studied the stability and reactivity of CH_2 species on Fe(110) in the presence of codeposited carbon and oxygen by using EELS. They concluded that the CH_2 species produced either through decomposition of ketene or diazomethane, is stabile and capable of remaining on the surface under UHV condition at 300 K for longer period. At temperatures above 400 K, changes in the CH_2 spectrum are observed. These changes are possibly due to the formation of an unstable vinylidene species through the interaction of CH_2 with surface carbon.

Zhou et al. [77] studied the decomposition of methyl iodide on the hexagonal close-packed Ru(001) using HREELS, AES, and TPD. They observed formation of the ethylidene (CCH_3(a)) species from CH_3I decomposition on metal surfaces. The adsorption and decomposition of acetylene on Ru(001) surface have been studied using HREELS and thermal desorption mass spectrometry [78]. Below 230 K acetylene is molecularly adsorbed on this surface with rehybridization of the acetylenic carbon atoms from an sp to a nearly sp^3 configuration. Between 230 and 250 K acetylene undergoes both dehydrogenation and hydrogenation reactions, resulting in the formation of two stable surface intermediates, ethylidyne (CCH_3), and acetylide (CCH) species. Both the ethylidyne and the acetylide decompose at a temperature near 350 K, accompanied by hydrogen desorption and leaving only methylidyne (CH) and carbon on the surface. The methylidyne decomposes with hydrogen evolution into the gas phase between approximately 480 and 700 K.

Goodman and coworkers [79–81] also observed hydrogen-containing species on Ru(001) and Ru(1120) single-crystal surfaces measured by HREELS. Methylidyne (Ru—CH), vinylidene (Ru—CCH_2), and ethylidyne

(Ru—CCH_3) species were observed on Ru(1120), while on Ru(0001) only methylidyne (Ru—CH) and vinylidene (Ru—CCH_2) species were observed in relation with the formation of higher hydrocarbons. Goodman also performed high-pressure experiments on the Ru single crystals and found that formation of carbonaceous intermediates is at an optimum at 500 K, while hydrogenation to ethane and propane took place at 400 K with optimum rate. When methane decomposition is carried out at above 700 K only the graphitic phase can be measured.

Steinbach et al. [82] studied the stability of CH_3, CH_2, CH, and C, species generated by adsorption and subsequent dissociation of CH_3Cl or CH_2Cl_2 on polycrystalline Co or Ni. XPS and ultraviolet photoelectron spectroscopy (UPS) were applied to characterize these surface species by assigning peak positions and temperature regimes for their existence. Due to the rapid dissociation of the C–Cl bond at the initial stage it is possible to generate $CH_{3(ads)}$ and $CH_{2(ads)}$ species. Temperature-independent peak positions over ranges of at least 50 K on Co and of about 40 K on Ni (see Table 6) indicate that the peak maxima used for identification are generated by the respective single species.

TABLE 6

Characteristic Binding Energies for the Species Adsorbed on Polycrystalline Co and Ni; Temperature Regimes Where a Species Is Visible and Dominant (in parentheses) [82]

	BE (eV)		
Species	XPS (AlK_α)	UPS (He(II))	Temperature, K
Cobalt			
CH_3	285.8	6.8–6.9	170–250 (150–300)
CH_2	284.9	5.5	(180–230)[a] 180–360[a]
CH	283.8	5.0–5.1	200–360 (190–450)
C	293.3	4.7	360–570
Nickel			
CH_3	285.6–285.8	6.5	170–210 (150–380)
CH_2	285.0–285.2	5.5–5.8	220–260 (180–420)
CH	283.8–284.0	5.2	270–470 (200–650)
C	283.5	4.3	480–850 (300–850)
C_1	268.9	5.8	180–850

[a]In CH_2Cl_2 experiments.

Schoots et al. [83] studied the dissociative chemisorption of methane on clean Pt(111). The results demonstrate that at an incident of normal kinetic energy (16 kcal mol^{-1}), methane adsorbs dissociatively on Pt(111) with an initial sticking coefficient of 0.06. This initial sticking coefficient for dissociative adsorption appears to be independent of surface temperature between 500 and 1250 K, implying that dissociation occurs via direct collisional activation rather than via trapping or precursor-mediated processes. The initial sticking probability for methane dissociative chemisorption on Pt(111) increases exponentially with incident normal kinetic energy. The activation energy for C–H bond rupture is 29 kcal mol^{-1}.

Henderson et al. [84] identified adsorbed methyl groups, $CH_{3(ads)}$, on Pt(111) after heating chemisorbed CH_3I to 260 K. The main desorption product of CH_3I decomposition on Pt(111) is methane. Photolysis of adsorbed CH_3Br on Pt(111) also generates adsorbed methyl groups, $CH_{3(ads)}$, on the surface and methane as desorption products [85,86]. Zhou and White [87] found that, for surface coverages up to one monolayer, the adsorption of methyl iodide is almost completely dissociative at 100 K, forming $CH_{3(ads)}$ and $I_{(ads)}$. Upon heating, low coverages of $CH_{3(ads)}$ decompose completely to $C_{(ads)}$ and $H_{(ads)}$ below 260 K, and there is no significant accumulation of $CH_{(ads)}$ or $CH_{2(ads)}$. For high coverages of $CH_{3(ads)}$, CH_4 is formed by the reaction of $CH_{3(ads)}$ with $H_{(ads)}$. On adsorption of CH_3I, C_2H_2I, and C_2H_5I on Pd(100) surface by photoinduced dissociation CH_3, CH_2 and C_2H_5 species were also stabilized [88].

Zaera [89] has provided spectroscopic evidence for the formation of both methyl and methylene groups on Pt(111) surfaces and has showed temperature-programmed desorption data which indicate that these intermediates can be hydrogenated to methane, even under low pressure. The product distribution for methane desorption after coadsorbing deuterium and normal methyl iodide also suggests that methylidyne (CH) moieties are formed on platinum surface.

Gesser et al. [90] studied dehydrogenative coupling of methane on a hot wire (1073–1173 K). A thermal diffusion column (TDC) produced higher hydrocarbons (30% conversion) which were separated and identified by gas chromatography–mass spectroscopy (GC–MS) techniques.

Under UHV conditions and on single crystals of VIIIB elements, CH_x could, therefore, be produced and stabilized and hydrogenated to hydrocarbons (mainly back to methane). Obviously, on single-crystal surfaces special conditions are required to stabilize CH_x species without decomposition to surface carbon. This process, however, is also a function of the nature of transition metals, whether they are noble or nonnoble VIIIB group elements.

V. SURFACE CARBONACEOUS SPECIES

In Sec. III it was clearly indicated that surface carbons of different reactivities can be formed when methane is adsorbed on metal surfaces. Sequen-

tial hydrogenation of surface carbon results in the production of CH_x surface species which can recombine to form C_{2+} molecules (see later). Apart from the initial steps, the sequence of the elementary surface reactions resembles those which we identified in CO hydrogenation. For the sake of better understanding, some relations between the surface intermediates important in methane coupling and CO hydrogeneration must be considered here.

Methane and CO yield surface carbon species of different properties. Normally, CO molecules dissociate more easily than methane and other saturated hydrocarbons. The nature of the carbon is, therefore, more or less predetermined: at relatively low temperature CO generates more reactive carbon species than methane, for which high temperature is required to dissociate. Nevertheless, the fate of carbon depends mainly on the metal used, the surface promoters, surface additives, etc.

Although formation of the surface carbon species has been well established from both CO and methane, we are not quite sure whether or not the reactive species formed from CO and methane, responsible for the further reactions, are identical. Namely, if methane starts dissociating, the step-by-step hydrogen abstraction might not end up at the completely dehydrogenated carbon species but at some intermediate state between CH_4 and $C_{(ads)}$; this state is the most populated one. Even, if it is so, this carbon is not necessarily the active intermediate, but it could be a "spectator" species. As can be seen later, the CH_x (where $1 < x < 3$) is the most likely be the active intermediate to form higher hydrocarbons.

On the other hand, in CO hydrogenation the active surface species have no other choice but to form carbon species first, then in successive hydrogenation CH_x species can be built up to serve as building blocks for the formation of higher hydrocarbons. This is why we have to briefly summarize the knowledge collected about the participation of various carbonaceous species in higher hydrocarbon formation.

Evidence has been presented [53,91,92] that, at least in the case of methanation, surface carbon is a probable intermediate; that is, CO dissociation preceded C–H bond formation.

Similarly to what was observed for two-step methane coupling, four types of carbon were observed by McCarty et al. [93] for CO dissociation over alumina-supported nickel methanation catalyst at 550–600 K. The order of their reactivity toward hydrogen the carbon species may be classified as: (i) chemisorbed carbon atoms, (ii) bulk nickel carbide, (iii) amorphous carbon, and (iv) crystalline elemental carbon. The α-phase and the initial monolayers of Ni_3C were much more reactive than the elemental forms as measured by temperature-programmed surface reaction in 1 bar H_2. At 550 K the α- and β-carbon species formed by CO exposure populate the surface with a ratio of about 2:1. Both phases are relatively stable on heating to 600 K in He atmosphere. At higher temperature, slow conversion of α- and β-carbon to graphite was observed. Hydrogenation of the α-state at 550 K leads to

methane at a sufficiently fast rate. This is the most likely intermediate in the nickel-catalyzed methane synthesis from hydrogen and carbon monoxide.

Biloen et al. [94] assessed the role of carbidic intermediates in hydrocarbon synthesis and they studied the incorporation of surface carbon into hydrocarbon products. Supported transition metal catalysts (Ni, Co, and Ru) have been precovered with carbon deposited via Boudouard reaction of ^{13}CO. Subsequent exposure of these catalysts to ^{12}CO and H_2 led to the abundant production of $^{13}CH_4$ and of hydrocarbons containing several ^{13}C atoms within one molecule. From this they conclude that oxygen-free species CH_x ($0 < x < 3$) are the possible intermediates for methanation, and that they were capable of being incorporated into growing hydrocarbon chains. Their results suggest that during CO hydrogenation, CO dissociated in a fast step to give carbidic intermediates from which both methane and higher hydrocarbons were produced.

Takeuchi et al. [95] observed that carbon atoms deposited on Rh/TiO_2 by the dissociation of adsorbed CO were extremely inert. These carbon atoms were not readily hydrogenated to form methane, methanol, or ethanol at 393 and 422 K. This result is in contrast to the behavior of supported Ni and Co samples, over which the surface carbon atoms deposited in a smaller manner are readily hydrogenated to hydrocarbons. There may be two possibilities to explain these results:

1. CO dissociates slowly at 523 K in the absence of H_2, and it therefore takes a long time to build up an appreciable amount of carbon on the rhodium. Due to the slow rate of formation, the deposited carbon may have sufficient time to be transformed into less active forms. Under reaction conditions in the presence of H_2, CO dissociation may be more rapid and the freshly deposited carbon may be more reactive.
2. The rate of CO dissociation is slow on Rh compared with that measured on Ni at 523 K. Therefore, the rate of CO dissociation might be so low around 423 K that CO undergoes hydrogenation preceding C–O bond rupture [52,96].

Only 50% of the ^{13}C deposited was ultimately hydrogenated to $^{13}CH_4$ at 573 K in the case of $^{13}C/Rh = 0.41$. The remainder was either unreactive (graphitic) or not directly associated with metal.

Bell et al. [50,97] showed that two distinctly different forms of carbon are present on the surface of Ru/SiO_2 catalyst. The two forms, designated as α- and β-carbons, exhibit quite different kinetics of formation and consumption. The surface coverage of α-carbon rapidly reaches a steady-state value. The steady-state rate of methane formation is found to be a linear function of the α-carbon coverage. The inventory of β-carbon is considerably larger than that of α-carbon and grows continually with time under reaction conditions. The β-form of carbon was less reactive than the α-form.

Studies on the surface coverage of unsupported ruthenium by carbon- and hydrogen-containing species during CO hydrogenation showed [98] that the coverage by adsorbed CO was close to a monolayer. Carbons α- and β-carbons were identified which differed in their dynamics of formation and conversion to hydrocarbons. The α-carbon is more reactive than β-carbon and is the principal intermediate in the synthesis of methane and C_{2+} hydrocarbons. The β-carbon accumulates continuously during the reaction but does not strongly inhibit the desorption of CO or hydrogen. A remarkable finding is that under reaction conditions, nearly one monolayer of hydrogen is adsorbed on the ruthenium surface. Additional hydrogen is found to be associated with the β-form of carbon, such that the H/C ratio of β-carbon was between 1.8 and 2.4.

Orita et al. [99] investigated the reactivity of surface carbon deposited on TiO_2- or SiO_2-supported Rh catalysts in the presence of molecularly adsorbed CO by means of the isotopic tracer technique and have made a direct comparison between the reactivity of adsorbed CO and that of surface carbon. They summarized that the activity of Rh catalysts in the disproportionation reaction depended upon the metal precursors and supports to a great extent. Rh/TiO_2 catalysts showed the highest activity, and the amount of surface carbon produced was larger than that of adsorbed CO. Three forms of carbon were identified, designated as α-, β- and γ-carbons: the first one was hydrogenated at temperatures up to 423 K and had a reactivity similar to that of adsorbed CO, the second one was oxidized to CO_2 at temperatures up to 473 K, and the third was the least reactive and was not oxidized at 473 K.

On rhodium catalysts the adsorption and dissociation of CO molecules at atmospheric pressure was investigated [51,100]. Dissociation was detected above 473 K. The carbon reacted with H_2 even at 300–473 K, yielding CH_4. A significant aging of surface carbon occurred above 573 K. Their results revealed that different kinds of surface carbon are produced by CO dissociation similar to the case for Ni [101]. The more reactive form reacts with hydrogen at 300–320 K and the less reactive one only above 600 K.

Existence of three types of carbon with different reactivities was directly proven by Lázár et al. [102]. On Fe/Cab—O—Sil and FeRu/Cab—O—Sil samples in situ Mössbauer spectroscopy showed formation of χ-carbide and reactive (or mobile) carbide; the latter is associated with iron with zero mm/sec isomer shift and 0.5 mm/sec quadrupole splitting, and is responsible for the higher molecular weight hydrocarbons formation. The latter form was present on both catalysts, while the formation of χ-carbide was suppressed on the ruthenium-containing sample as an effect of the modifier action of ruthenium. Further catalytic studies indicated that C_{2+} formation stopped when the CO stream was disconnected, but methane was still formed and simultaneously the Fe–C species with 0.5 mm/sec quadrupole splitting disappeared. From these experiments the existence of the following was suggested: (i) reactive (or mobile) carbide which is responsible for C_{2+} formation and corresponds to α-carbon, (ii) surface carbon from which methane is pro-

duced at the reaction temperature (probably β-carbon), and (iii) inactive or strongly bonded carbon (χ-carbide) which can be removed only by oxidation.

It is, therefore, well established that in the interaction of CO and CH_4 with metal surface, carbon species of different reactivities (α-, β-, and γ-carbon) are formed. Among these species α-carbon appears to be the most reactive species, capable of further surface elementary reaction reactions. The reason why the carbon formed from CO is more reactive than that formed from CH_4 (see later) is not clear yet. Beyond the classification of these species we have not much knowledge about how its reactivity and stability depend on the particle size, the support, acidity, promoters, etc.

The carbide/carbene mechanism was known earlier [103,104] but evidence for this was obtained only recently. Ekstrom and Lapszewicz [105] have shown that high molecular weight hydrocarbons can be formed by the reaction of carbides with hydrogen in the presence of water. Insertion of CH_4 into propene on Ni has recently been reported [106].

The most convincing supports for the carbide/methylene mechanism resulted from the elegant studies carried out by several research groups. The use of different —CH_2- or —CH_3-containing probe molecules, such as alcohols [107–109], open-chain olefins [110–112], cycloolefins [112,113], CH_2N_2 [114], alkylhalides [115,116,119], and nitro paraffins [107,117,118], offered the most spectacular results to supply evidence for the participation of CH_x species in chain lengthening.

Decomposition of CH_2N_2 [114] on Ni, Pd, Fe, Co, Ru, and Cu surfaces at atmospheric pressure in the temperature range of 298–523 K produced only ethylene and dinitrogen. This indicates that in the absence of hydrogen the absorbed —CH_2— fragments dimerized to ethylene, but polymerization to higher hydrocarbons did not occur. Cavalcanti et al. extended their studies for the use of CH_3NO_2 as probe molecules in the study of CO hydrogenation over Ru/KY [117] and Ru/SiO_2 [118] catalysts. The formation of the higher hydrocarbons increased upon CH_3NO_2 addition without significant changes in the carbon fraction distribution due to the incorporation of CH_x groups derived from CH_3NO_2, as shown in Table 7.

Van Barneveld and Ponec [116] also confirmed the participation of —CH_x— in the formation of hydrocarbon chains using chlorinated methane molecules in mixtures with H_2 or with H_2 and CO on metals (Ni, Co, Cu, Fe, Rh, Pd) and on some alloys (Ni–Cu, Ni–Pd). It appeared that metals active in the FT synthesis produced higher hydrocarbons both in the absence and in the presence of carbon monoxide.

Theopold and Bergman [120] showed that a bridging CH_2 ligand in $CH_2CO_2(CO)_2$—$(C_2H_5)_2$ reacted with ethylene to yield propene.

Here we have to report on the work in which methane can also be a source of the —CH_2— species. Tanaka et al. [121] suggested that the —CH_2— species formed on cobalt catalysts were the most important precursors for the formation of higher hydrocarbons. They created CH_2 fragments by dissociative methane adsorption at 703 K on 6.0 wt% Co/Al_2O_3, 14.7 wt%

Co/C as catalysts. The nature of the reactive species deposited was identified by deuterium-labeling experiments at 703 K. The results suggested the presence of reactive species such as CH_2, although it was only a small portion of the deposited carbon on cobalt catalysts. To confirm the presence of CH_2 species, they performed the following experiments:

- Ketene (CH_2—C═O) was decomposed on the 6.0 wt% Co/Al_2O_3 catalyst at 723 K, followed by treatment with deuterium at 703 K. The deuterium distribution in the methane obtained was similar to the results obtained from the decomposition of methane and carbon monoxide.
- CD_4 was decomposed at 703 K and hydrogenation of the species on the catalyst with H_2 gave CD_4 and CD_2H_2. This result suggested the formation of CH_2 or CD_2 species on cobalt catalysts by the decomposition of CH_4 or CD_4.

Insertion of the CH_2 species into ethene was confirmed by the isotopic distribution in the methane and ethylene obtained in the hydrogenation of ^{13}C deposited Co/C catalyst at 703 K with 8.65 kPa of H_2.

Methane (%)			Ethylene (%)	
$^{12}CH_4$	$^{13}CH_4$	$^{12}C_2H_4$	$^{12}CH_2{=}^{13}CH_2$	$^{13}C_2H_4$
69	31	1	32	67

Here 31% ^{13}C was observed in methane compared with 83% in the ethylene.

Tanaka has also found that the reaction of $^{12}C_2H_4$ with ^{13}C deposited on cobalt catalyst yielded propene containing one ^{13}C atom, which supported the metallacyclobutane mechanisms proposed for the homologation reaction.

In the literature a few surface science oriented experiments can be found

TABLE 7

Product Distributions CO Hydrogenation Over Ru/KY in the Presence and Absence of CH_3NO_2 [117]

	Condition A		Condition B	
C fraction	Without CH_3No_2	With CH_3NO_2	Without CH_3NO_2	With CH_3NO_2
C_1	38.9	41.8	156.5	165.4
C_2	15.0	25.0	38.0	48.1
C_3	30.3	46.4	74.4	91.3
C_4	21.4	29.0	44.9	53.9
C_5	17.0	24.8	31.3	39.4
C_6	10.1	12.9	16.4	18.6
Total	132.7	179.9	361.5	416.7
CO conv.%[a]	1.1	5.9		

[a]CO conversion into hydrocarbon products.

which provide evidence for the —CH_2— species being a key intermediate in the higher hydrocarbon formation. Here the problem is the higher reactivity of the clean surface, on which it is difficult to retain a stable C–H bond as dissociation easily proceeds to bare carbon atoms. Nevertheless, Kaminsky et al. [63] already reported the moieties of CH, CH_2, and CH_3 intermediates on a Ni(111) methanation catalyst.

The use of CH_3NH_2 and CH_3NO_2 as probe molecules adsorbed over Pt(111) does not give correct results either, because of the high stability of C–N bond Nonetheless, Hwang et al. examined the decomposition of CH_3NH_2 on Pt(111) [122] and also the decomposition and oxidation of CH_3NH_2 on polycrystalline platinum wires [123] at higher pressures. They found that the C–N bond in CH_3NH_2 was very stable on Pt(111), and no significant C—N scission was observed with TPD up to 1250 K [122]. Even addition of oxygen over Pt wires at 1450 K did not significantly change the decomposition chemistry of the C–N bond in CH_3NH_2 [123] while excess O_2 was present. Furthermore, Hwang et al. [124] also studied the adsorption and decomposition of CH_3NO_2 on Pt(111) using TPD, XPS, and AES. The major decomposition path of the adsorbed CH_3NO_2 on Pt(111) was the dissociation of C–H bonds and N–O bonds to leave an adsorbed CN group which desorbed as C_2N_2 between 750 and 1200 K. Hence Pt(111) had a surprising inability to break the C–N bonds, in spite of its relatively low bond energy. Thus, platinum appeared to be both very reactive and highly selective for organic molecules containing nitrogen. This appears to arise from the ability of platinum to form a C–N triple bond which is very stable and does not dissociate.

We have to conclude that the participation of the CH_2 species in the CO hydrogenation reaction to form higher hydrocarbons is unambiguous. In the correlation between methane coupling and CO hydrogenation, this species can be regarded as the key intermediate.

VI. NONOXIDATIVE METHANE COUPLING REACTIONS

Nonoxidative methane conversion into higher hydrocarbons is one of the recent achievements in research on methane coupling. Here the idea is to separate the two steps by temperature and time, with the first being methane decomposition on metal at high temperature followed by hydrogenation of the surface carbonaceous species at lower temperature. Van Santen et al. [29,125–129] studied the low-temperature two-step methane conversion route toward C_{2+} (from ethane to pentane) hydrocarbons on silica-supported ruthenium, rhodium, and cobalt catalysts. Around 632 K, the methane is dissociatively adsorbed on a cobalt catalyst, resulting in hydrogen and surface car-

bonaceous species. Subsequently carbonaceous intermediates is able to produce small alkanes upon hydrogenation at 373 K:

$$2CH_4 + 6Co \rightarrow 2Co_3C + 4H_2 \qquad \text{at 632 K}$$

$$2Co_3C + 3H_2 \rightarrow C_2H_6 + 6Co \qquad \text{at 373 K}$$

Separation of the two steps was necessary because the thermodynamic analysis showed that, for example, on cobalt, which was one of the most efficient catalysts, $\Delta G°$ was zero at 370 K and 650 K for $2Co_3C + 3H_2 \rightarrow C_2H_6 + 6Co$ and $2CH_4 + 6Co \rightarrow 2Co_3C + 4H_2$, respectively (illustrated in Scheme 1).

As was indicated earlier [29], three types of carbon form on the surface: surface carbide (α-carbon), amorphous carbon (β-carbon), and graphite (γ-carbon). The last one is totally inactive, hence its participation in the reaction is highly improbable. The most reactive was the α-carbon which can form higher hydrocarbons or participate in chain lengthening (homologization), as is shown for the reaction between α-carbon and pentene pulses.

In the Eindhoven group, ruthenium finally proved to be the best catalyst and in recent work they increased the activity of the 5 wt% Ru/SiO_2 prepared by incipient wetness impregnation from $RuCl_2$ [130]. After reduction in hydrogen, the catalyst was additionally treated with CO, and due to this treatment, the chemisorption capacity increased. Simultaneously the carbon monoxide dissociation also increased. These effects could be attributed to structural changes resulting in larger metal ensembles. The catalytic activity of this sample is not known yet.

Support effects were investigated in the two-step methane conversion

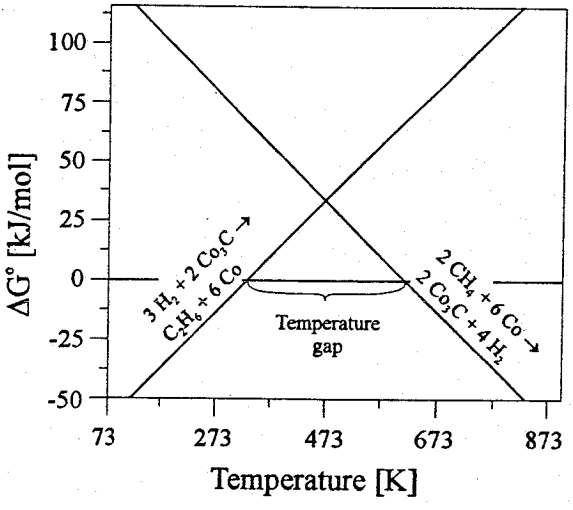

SCHEME 1.

over ruthenium catalysts by Cheikhi et al. [131]. Various supports, such as Al_2O_3, $AlPO_4$, and $Zr_3(PO_4)_4$, were applied, and zirconium phosphate proved to be the most effective based on the conversion per gram of ruthenium metal. It was interesting to learn that for both methane adsorption and hydrogenation, the same temperature was used and the fraction of higher molecular weight products increased with increasing adsorption and hydrogenation temperature. Metal dispersion changed from support to support; however, with one support the activities, expressed in turnover frequency (TOF), were found to decrease with increasing metal dispersion.

The interaction of Ir/SiO_2, Ir/Al_2O_3 Ir/TiO_2, and Ir/MgO with methane at 473 K yielded hydrogen, ethane, and carbonaceous species. With increasing temperature up to 773 K the conversion varied between 2% and 5%, with MgO being the best support. FTIR results indicated that CH_3 was the reaction intermediate. In the subsequent hydrogenation, hydrocarbons up to hexane were produced [132].

Platinum also appeared to be an efficient catalyst in methane coupling. In contrast to the previous works, here the one-step process for C_{2+} formation was applied in which a very low yield was observed and catalyst activity was lost after a few second [133–135]. On Pt catalyst methane was decomposed via continuous-flow adsorption and the resulting surface intermediates were hydrogenated at the methane decomposition temperature.

Belgued et al. [133] reported the production of higher hydrocarbons from methane over EUROPT-1 by using a two-step reaction sequence. In the first step, 100 mg of EUROPT-1 (a standard platinum catalyst in European catalysis laboratories [136]) was exposed to pure methane with a flow rate of 400 cm^3/min at 523 K. They observed ethane evolution (52.8×10^{-8} mol) with a selectivity of 63.5%, which is equal to 40% of the amount of C_2H_6 formed in the reaction of $2CH_4 \rightarrow C_2H_6 + H_2$ (8.6×10^{-6} mol) at equilibrium. The total amount of methane converted was 19.3% ($= 1.66 \times 10^{-6}$). It increased to 29% when the whole process was conducted at 473 K, but the corresponding amount of higher hydrocarbons produced was lower (1.05×10^{-6} mol) as less methane was adsorbed during the exposure. The key factor of success in their experiments was the continuous removal of the hydrogen by the flow of methane during exposure.

These results were compared with those obtained on ruthenium and cobalt at low temperature (523 K) [134]. On the basis of adsorbed methane, the yields of C_{2+} hydrocarbons amounted to 19.3% on platinum at 523 K, to 36.9% on ruthenium at 393 K, but only 7.5% on cobalt at 543 K. The distribution shifted toward products of higher molecular weights at higher temperatures on platinum, but Co and Ru displayed an opposite trend. Strikingly, on Ru the pentanes were the most abundant products at 393 K (39.8%). The conversion of the absorbed methane and the distribution of the products were strongly influenced by the flow rate of methane during the exposure. The product distribution was significantly affected by the flow of hydrogen; that is, at 573 K with hydrogen flow rate 50 cm^3/min, the C_2 selectivity on cobalt

catalyst is 84.8%; but at a hydrogen flow rate 300 cm^3/min, the C_2 selectivity decreased to 66% but selectivity to C_3, C_4 products increased.

Considerable improvement was achieved by the work of Pareja et al. [137]. They established that during methane adsorption on EUROPT-1 the hydrogen evolved was removed, with most of the methane not being adsorbed on the catalyst. Therefore, a hydrogen trap containing 5 wt% Pd on alumina working at room temperature was attached to the adsorption loop and during methane adsorption hydrogen was trapped. Using this device the conversion of methane to higher hydrocarbon increased to about 40% measured at 523 K, and the distribution of C_{2+} products shifted toward higher hydrocarbons if the exposure time increased from 3 to 16 min (Table 8).

Mielczarski et al. [138] reported that platinum-loaded zeolites (Pt/HX and Pt/HY) play an interesting role in the conversion of methane into higher hydrocarbons. They observed that the total amount of desorbed hydrogen was much larger than that of ethane, indicating the occupation of CH_x species ($x < 3$) on the surface. On Pt/HX there was no change in the yield of higher hydrocarbons between 523 K to 598 K, whereas on Pt/HY there was a decrease in the yield of higher hydrocarbons (Table 9).

As far as the activity of the catalyst was concerned, Pt/HX is more active than Pt/HY and EUROPt-1. More methane homologation was observed on Pt/HX than Pt/HY and EUROPt-1. If the catalysts are compared, the reactivity

TABLE 8

Comparison of the Various Pt Samples in Methane Coupling [137]

Catalyst	Amount of CH_4[a]	Selectivity (%)				
		C_2	C_3	C_4	C_5	C_6
Pt/HX	1.98	39.9	18.8	19.6	19.6	2.1
Pt/HY	1.52	38.5	31.4	22.9	6.2	1.0
EUROPT-1	1.22	75.0	13.2	0.9	10.1	1.0

[a]Amount of the CH_4 used up for homologation, expressed in mmol.

TABLE 9

Comparison of the Various Zeolite Supports in CH_4 Conversion

T, K	CH_4 (ads)[a]		CH_4 conv		Yields (%)[b]	
	HX	HY	HX	HY	HX	HY
523	3.6	2.9	1.4	1.5	39	52
598	6.1	4.7	2.4	1.4	39	30

[a]The amounts of methane expressed in mmol. Conditions: sample, 100 mg; step 1, exposure to methane (1 atm, 200 cm^3/min, 30 sec); step 2, exposure to hydrogen (1 atm, 50 cm^3/min, 5 min).

[b]Defined in carbon adsorbed.

as well as the adsorption of methane was greater on Pt/HX than on Pt/HY. This result might be attributed to the difference in acidity and different electronic states of the Pt supported on these zeolites. Hydrogenolysis studies revealed that Pt/HY was more acidic than Pt/HX.

According to Besouhanova et al. [139], platinum in acidic zeolites is electron deficient, whereas it is electron rich in alkaline zeolites. According to Gallezot [140], and Sachtler et al. [141], it was found that metal–support interaction leads to charge transfer from the zeolite to the cluster. The decrease in acidity results in a greater electron density on small metal particles within the zeolite pore. IR diffuse reflectance spectroscopy also indicated that small Pt particles encapsulated in NaX zeolites have unusual properties. The wavenumber of the metal—carbon stretching frequency of the adsorbed CO shifted 60 cm^{-1} toward higher values compared to that measured on large Pt particles [143]. The stronger bond can be ascribed to a negative charge on the small metal particles.

This was further supported by quantum-chemical calculation of Jansen and van Santen [142]. They reported a Hartree–Slater–Foch linear combination of atomic orbitals (HSF-LCAO) calculation for chemisorption of CO, H_2 over small Ir_4 clusters in the presence of a Mg^{2+} ion normally located in zeolite cages. The CO adsorption was strengthened when the iridium cluster was sandwiched by Mg^{2+} and CO, whereas the opposite was observed in the case of hydrogen.

The use of zeolite undoubtedly appears to be an attractive application in methane coupling. Recently, HZSM-5 was also applied with or without metal insertion (Mo, Zn, Pt, and Fe) [144,145]. Methane and ethane at 873 and 823 K temperature, respectively, were dehydrogenated and after coupling, aromatic compounds were formed. This is a promising area for the future application. Pb and Cu modified SAPO-5, ALPO-4, and ALPO-5 have also been used to activate the C–H bond in methane, and the methyl radicals produced were added to aromatic compounds [146]. At 673 K and at 6.9 bar pressure, the aromatic conversion lay in the range of 1–21%, with a selectivity for aromatics of about 40%. The selectivity for xylenes rose to between 70% and 90%.

In nonoxidative methane coupling only one application is known in which nonmetal components but different supports are utilized [147]. Above 1123 K alumina among MgO, SiO_2 appeared to be the most active sample, with 25–28% conversion for C_{2+} and 60–70% selectivity. The temperature applied, however, proved to be too high for this application.

In all the experiments described so far, one of the major problems is the extraction of hydrogen from methane and the removal of hydrogen from the surface. This is why a membrane reactor was used for a process in which no direct oxygen contact with methane took place. The basic idea was described as follows [1,148]:

$$2CH_4 + MO_x \rightarrow C_2H_6 + H_2O + MO_{(x-1)}$$

$$MO_{(x-1)} + 1/2O_2 \rightarrow MO_x$$

That is, reducible oxides were used, such as PbO, Tl_2O_3, Sb_2O_3, MnO_2, or

SnO_2, to create a catalyst. Hydrogen was abstracted by these catalysts and then the catalyst was reoxidized in a separate cycle. This idea was applied for a membrane reactor in which the membrane wall was constructed of PbO modified alkaline and an alkaline earth compound supported on porous SiO_2–Al_2O_3 tube. Outside the porous tube, methane was introduced, while inside the tube a stream of oxygen was flowing. Using the oxygen ions of PbO, the hydrogen from methane was abstracted, water was formed, and then partially reduced PbO was reoxidized with oxygen diffusing through the porous wall. In this way the CH_4 conversion rate was 0.5×10^{-4} mol s^{-1} m^{-2} with nearly 90% C_{2+} selectivity.

Other hydrogen acceptors were also tried. Titanium [149] or silver [150] were applied with the idea that titanium easily forms titanium hydride and atomic oxygen could diffuse easily through the silver membrane. Although the idea is excellent, the major drawbacks are, for titanium, the easy formation of TiC from ethane formed and the total oxidation of the hydrocarbon, in the case of silver.

VII. MECHANISM OF CH_x FORMATION OVER METAL SURFACE

Here we report some attempts which describe the mechanism of methane coupling. Isotope tracing techniques were applied to explore the mechanism of methane coupling. On Pt, Pd, and Ni catalysts CH_4/D_2 and CH_4/CD_4 isotope exchange reactions between 523 K and 673 K were examined [152]. CH_4/CD_4 exchange started at 473 K, with Pd being the most active for C–H and C–D bond cleavage. In the absence of oxygen the reaction was reversible, whereas in the presence of oxygen total combustion took place on Pd at 573 K with only a minute amount of C_2 formation. The same research group also applied the isotope method for transient kinetic measurements [151]. On alkali carbonate promoted lanthana and MgO samples, one monolayer of methane was deposited which adsorbed in the reversible mode. On basic sites heterolytic splitting was assumed via the intermediate of $CH_3^{\delta-}$–$H^{\delta+}$. Simultaneously the amount of surface intermediate leading to higher hydrocarbon was very small. By these experiments they explained the role of alkali promoters; namely, by neutralizing most of the strong acid sites on the surface, the carbonate layer that was formed in the presence of oxygen inhibited the further reaction of methyl radical precursors to CO and CO_2, thus C_2 selectivity increased. Using the same method Driscoll et al. came to the same conclusion for the mechanism and the role of the alkali promoter for methane coupling over $MnMoO_4$ catalysts [154].

Ga- and Zn-exchanged H-ZSM5 catalysts were applied in isotope exchange experiments between perdeuterated and nondeuterated hydrocarbons (CD_4–C_3H_8, C_3D_8–C_3H_8) studied by Iglesia et al. [153]. Alkane conversion took place slowly because the rate limiting step was not the C–H

bond activation but the disposal of H atoms formed in the C–H bond cleavage. Coupling of the C–H activation with H-transfer to acceptor sites often increases the alkane activation rate.

One of the most intriguing problems is to determine the number of hydrogen atoms in the CH_x species. This has also been studied by the isotope method [155]. After methane deposition on Ru, Co, and Pt metals supported by alumina and silica, dideuterium was applied in place of hydrogen to remove the CH_x species in the form of $CH_xD_{(4-x)}$. After careful calculations (taking into account the fragmentation correction and the naturally occurring ^{13}C), the distribution gave an estimation on the "extent of dissociation" of methane. Ruthenium proved to be the most aggressive metal to remove hydrogen, whereas Pt is not too active. This was the most likely explanation why Pt was more efficient for the formation of higher hydrocarbons than, for example, Ru. On Co the formation of surface carbonaceous deposit took place to the greatest extent.

VIII. LOW-TEMPERATURE METHANE ACTIVATION WITH HOMOGENEOUS CATALYSTS

There is growing interest in homogeneous activation of methane to convert it into liquid products at ambient temperature. It is known that the C–H bond can be activated heterolytically at low temperature with the application of homogeneous catalysts. The process is always linked with partial oxidation of methane, resulting in the formation of methanol or methyl chloride, but not in hydrocarbon production. Nevertheless, this process may have a large industrial impact in the future; thus we feel that it is worthwhile reviewing here.

It has been known for a long time that methane can be oxidized at 393 K and at 6 bar pressure in the presence of H_2PtCl_5/Na_2PtCl_4 to form methanol and methyl chloride [156]. Similar results were obtained with the use of palladium propionate dissolved in trifluoroacetic acid (TFA) at 363 K and 6 bar pressure. Here TFA methylester was formed [157].

Nelson and Foger [158] studied the electrophilic activation of methane in TFA using Pd, Pt, and Co compounds. The detailed mechanism showed that the reaction took place at 423 K and 5.5 bar according to the following mechanism:

$$Pd(II)(O_2CCF_3) + CH_4 \rightarrow H_3CPd(II)(O_2CCF_3)$$

and then by reductive elimination

$$H_3CPd(II)(O_2CCF_3) \rightarrow Pd(0) + CH_3O_2CCF_3.$$

Labinger et al. [159,160] followed the work of Shilov [156] using Pt(II) and Pt(IV) complexes. In their experiments they observed decreasing

methanol selectivities with increasing methane conversion (100 to 60% and 0.2 to 5%, respectively).

Nakata et al. [161] carried out a series of experiments with the activation of C–H bonds in methane, ethane, and propane. With CO and methane mixture at high pressure, methane could be functionalized to produce acetic acid in the following equation:

$$CH_4 + CO \{\text{in presence of Cu(II), } K_2S_2O_8/TFA\} \rightarrow CH_3COOH$$

Coordinatively unsaturated iron complex $HFe(CO)_n^+$ or η^5-$C_5H_5(CO)_2Fe$ formed adducts with methane [162]. The possible mechanism involved elementary steps in which the metal was inserted into the C–H bond followed by β-elimination of hydrogen.

An excellent review was given about the homogeneous activation of C–H bonds at low temperature in the presence of homogeneous catalysts by Crabtree [163–165]. Electrophilic attack of the C–H bond is the simplest approach and since methane was the least basic alkane, superacid conditions are required: $CH_4 + E^+ \rightarrow CH_3^+ + EH$.

The most promising approach was discovered in 1993 by Periana et al. [166,167]. Here a novel, homogeneous system for the selective, catalytic oxidation of methane to methanol via methyl bisulfate was introduced. In presence of mercuric ions, Hg(II), concentrated sulfuric acid methyl bisulfate, water, and SO_2 are formed at 373 K and at 18 bar, with a 50% methane conversion and 85% selectivity to methyl bisulfate. The Hg(II) turnover frequency is 10^{-3} s^{-1}. In a separate step methyl bisulfate was hydrolyzed and

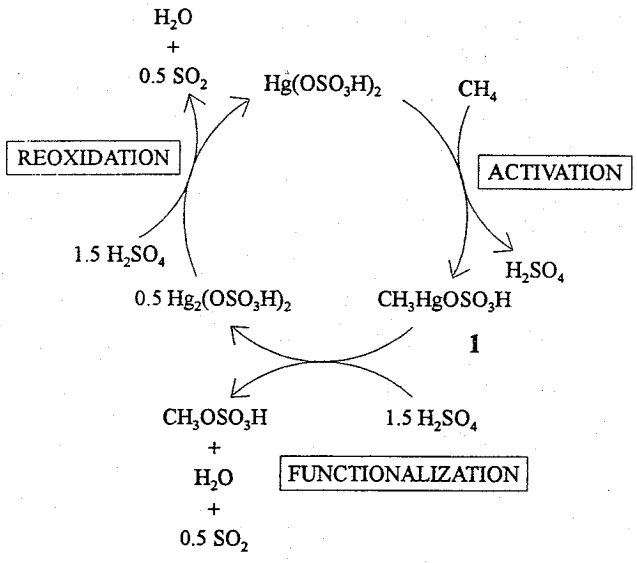

SCHEME 2.

sulfur dioxide was reoxidized by air. In the first step methane reacted with Hg(II) ions via an electrophilic displacement mechanism to produce CH_3HgOSO_3H, which decomposed readily to CH_3OSO_3H and Hg_2^{2+}. Tl(III), Pd(II), platinum, and gold were also candidates for catalytically active ions. The full mechanism is presented in Scheme 2.

IX. METHANE ACTIVATION WITH CO_2

Another promising route toward methane activation in which oxygen molecules do not directly participate should also be mentioned here. There is already an existing plant in which methane and carbon dioxide are converted into a mixture of CO + H_2 at a cost of US$137.00 to produce 1 ton of CO [168]. Although methane reforming with CO_2 becomes a major problem due to the gradual increase of CO_2 in the natural gas wells as they become exhausted, here we report only on some recent results [169–172] which might be relevant to the future process.

Mainly Ni [169–172], Pt [171], and Rh [170] as catalysts were examined, with special attention being paid to catalyst deactivation, support effect, and new composite catalysts [172]. Since the reaction occurred at around 973–1123 K, carbon deposition seemed to be a very serious drawback in this application. Normally, alumina-supported catalysts were easily coked; application of ZrO_2 as support considerably improved the catalyst performance at long range [171]. A similar effect was reached with $Ni_xCa_yMg_{(1-x-y)}O$ composite catalysts [172], which showed negligible deactivation even after 100 h time on stream. On the other hand, the catalyst activity was found to be controlled primarily by the nickel phase (dispersion and the extent of reduction) and only to a small extent by the support and additives [169]. Nevertheless, in the future this process could be feasible, just like methane partial oxidation to CO and hydrogen [173].

X. REACTIONS OF SURFACE CH_x SPECIES WITH HYDROCARBONS

Reaction of CH_x species with other hydrocarbons is one of the most intriguing parts of methane chemistry. When an on-surface-generated C_1 species starts reacting, higher molecular weight products from CH_x species by surface polymerization process are being built up. This reaction has its own regularities, which are reviewed in this section.

Löffler et al. [174] reported that methane reacted with unsaturated compounds under heterogeneous gas phase conditions. Up to 7% toluene was formed by the reaction of methane with benzene at 573 K on a Ni/SiO_2 catalyst at atmospheric pressure. This was the reverse of technical benzene production by hydrogenolysis of toluene. In control experiments using argon

as the carrier gas instead of methane, only benzene was recovered. The addition of methane to an olefinic C–C double bond was exothermic at lower temperatures. The reaction of methane with cyclopentene at 583 K and atmospheric pressure (with a 20% Ni in sodalite) gave benzene in 33% yield, and smaller amounts of toluene (9%) and cyclopentane (13%). Control runs with nitrogen carrier gas yielded only 5% benzene, demonstrating the effect of the methane. Higher pressure (up to 10 bar) experiments, which allowed higher surface occupation, gave mostly cyclopentane and very little benzene. The reaction of methane with methylenecyclopentane gave a yield of toluene up to 23% at 573 K and 1 bar. The reaction of methane with the alkene must precede aromatization, for example, conversion of methylenecyclopentane into benzene. Further studies showed that ethene, propene, and the butenes reacted in the presence of methane and on methane-reduced nickel catalysts to form complex mixtures of hydrocarbons. A methane/propene gas mixture (containing 6% propene) was passed over 7.5% Ni on silica at 603 K and 10 bar. The resulting product composed of 53% C_1, C_2, 26% C_3H_8, 8.5% C_4H_{10}, and 13% C_5, C_6 hydrocarbons indicated methane consumption. In the control experiment using nitrogen instead of CH_4, the product composition was different. Methane apparently formed active CH_x–nickel species during reduction of the catalyst and these combined with unsaturated substituents. When an inert carrier gas was employed, some of the carbonaceous species were removed from the surface and this resulted in lower yield of the higher hydrocarbon.

Van Santen and coworkers [175] adsorbed methane on silica-supported Ru and Co at 600–800 K; then after cooling down, olefins were coadsorbed and as a result of hydrogenation, carbon–carbon bonds were formed. The mechanism was related to that found for homologation from other sources.

Tanaka et al. [176] presented a mechanistic relation between hydrogenolysis and pentene transformation to butene and hexene over Ru/SiO_2 catalyst. Labeling experiments confirmed that the terminal olefin was cleaved at the double bond to yield labeled C_1 fragments at low temperature; then it was incorporated in the starting terminal alkene molecules to produce higher homologues. This C_1 fragment was only slightly hydrogenated to methane. Both C–C bond formation and cleavage could be explained by a ''carbene insertion–abstraction mechanism'' to a metal–alkyl fragment.

Dissociative methane adsorption on transition metal surface had a low sticking coefficient. Under mild conditions alkenes had a very high sticking coefficient with respect to transition metal surfaces. Mainly for these reasons, direct coupling of alkenes with methane catalyzed by transition metals has not yet been realized, while indirect conversion routes have very low selectivities [177]. Using solid superacids under mild conditions, methane has been shown to add to ethylene selectively as long as a high methane/ethylene ratio was used in order to suppress ethylene oligomerization [178].

Van Santen et al. [129,179] reported a chain increase of alkenes with methane catalyzed by Group VIIIB transition metals. First, methane is ad-

sorbed dissociatively to a previously reduced transition metal catalyst at 723 K. After methane deposition the catalyst was quickly cooled in a helium flow to prevent "aging" of the surface carbon. In a second step an alkene was coadsorbed onto the methane-treated catalyst. Then, the system was exposed to hydrogen and hydrocarbons desorbed. The catalysts studied are 5 wt% Ru/SiO_2 and 10% Co/SiO_2 prepared by incipient wetness impregnation. When propene was coadsorbed, methane formation was reduced and butane formation increased. This might be indicative of reaction between carbon from methane and adsorbed propene to butane. In order to distinguish disproportionation from the incorporation of carbon from methane, experiments were performed with ^{13}C-labeled CH_4. The percentage of the reaction products, formed at 323 K and 1 bar H_2, consisting of one ^{13}C-labeled carbon atom from methane and ^{12}C atoms from preadsorbed ethene or propene, are presented in Table 10.

From these experiments it was shown that methane was incorporated into the reaction products. From fragment mass spectra they concluded that the ^{13}C atom appeared as the primary carbon atom in the product propane and butane. Since nearly half of the homologated product molecules were due to self-homologation, the reactivity of surface carbon from methane was very similar to that of surface carbon generated by hydrogenolysis of alkenes.

The mechanism of C–C bond formation between the adsorbed carbonaceous surface species was closely related to that occurring in the FT reaction in which mainly linear products were formed. This conclusion supported the findings of Tanaka et al. [180,181], who indicated that addition of potassium to an MoO_x/SiO_2 catalyst greatly enhanced alkene metathesis activity with extremely good selectivities. Later, they showed [182] that homologation reaction (carbon scrambling occurs) was independent of the metathesis reaction.

When the mechanism is clarified, attention must also be paid to the C–C bond cleavage. Namely, it is well known that Ni is an excellent catalyst in the hydrogenolysis of saturated hydrocarbons. At high hydrogen-to-hydrocarbon ratios selective C–C bond rupture takes place at the terminal position (α-splitting) but under hydrogen-deficient conditions, "deep" fragmentation prevails [182] resulting in the formation of methane. During this fragmentation CH_x is also formed which might participate in the chain build-

TABLE 10

Carbon Atom Insertion Over Various Catalysts [179]

	Catalyst	
Reaction	5% Ru/SiO_2	10% Co/SiO_2
$^{13}CH_4 + C_2H_4 \rightarrow {}^{13}C^{12}C_2H_8$	60%	62%
$^{13}CH_4 + C_3H_6 \rightarrow {}^{13}C^{12}C_3H_{10}$	45%	73%

up. This gave an explanation for the formation of toluene from *n*-hexane which was observed on a Ni black sample [183].

Detailed tracer studies have elucidated the mechanism of this reaction [184,185]. First, the route of disproportionation of *n*-hexane to form *n*-pentane + *n*-heptane followed by dehydrocyclization of *n*-heptane to toluene was excluded. The remaining choice was that first *n*-hexane was dehydrocyclized to benzene and, then, the benzene was alkylated by a C_1 unit formed on nickel catalyst.

Using labeled ^{14}C-methane or -propane, the toluene did not pick up labeled carbon. Hexane was not the source of the C_1 unit, either. From these experiments it is concluded that high temperature is required to activate methane and other hydrocarbons to produce C_1 units. Contrary to the results observed over supported nickel catalysts, on unsupported nickel the methane decomposition, if any, yielded unreactive surface carbon which was unable to react with benzene. This was also the case for higher molecular weight hydrocarbons, like propene and hexane.

Further experiments, however, demonstrated that the source of C_1 units was benzene which was partly decomposed during its formation. Using ^{14}C-C_6H_6 as a labeled intermediate and an *n*-hexane mixture, the following results were obtained (Table 11). If the source of C_1 unit were not the benzene, the specific isotope content of toluene (millicuries/millimole) would have been lower than the corresponding value for benzene. If benzene were the source, the specific isotope content of benzene and toluene would be equivalent during the reaction: ^{14}C-benzene is diluted by ^{12}C-benzene (from hexane), but when it is partially decomposed to the $^{14}C_1$ unit its specific radioactivity is not affected. As Table 11 shows, the specific radioactivities of benzene and toluene run in parallel way, so the benzene route is valid. These experiments well illustrate that methane activation—or more generally,

TABLE 11

Radiotracer Study with ^{14}C-Labeled Benzene on Benzene–Toluene Reaction at $p_{H2}/p_{hex} = 4.6$ and at Different Temperatures [185]

	Temperature			
	616 K		637 K	
Time	ρ_B/ρ_B°	ρ_T/ρ_B°	ρ_B/ρ_B°	ρ_T/ρ_B°
0	1	—	1	—
15	0.91	1	0.83	0.90
30	0.86	0.98	0.83	0.90
60	0.83	0.96	0.67	0.83
90	0.68	0.83	0.44	0.44

Note. ρ_B°, ρ_B, and ρ_T are the specific radioactivities (mCi/mmol) of benzene (initial), benzene at time *t*, and toluene at time *t*, respectively.

small saturated hydrocarbon decomposition—is a rather inefficient process, at least on unsupported metal catalyst.

Nevertheless, chain-lengthening reactions—that is, interaction between methane and hydrogen acceptor molecules, for example, olefins—were thermodynamically favored. Schleyer et al. [186] reported that methane reacted with benzene, cyclopentene, and propene to produce small amounts of toluene, methylcyclopentane, and butanes, respectively, using silica-supported nickel catalysts. Presence of the carbonaceous species on catalytic surfaces was depicted by XPS studies.

Scurrell [177,187] reported that a mixture of methane and ethene reacted over sulfate-treated zirconia catalysts to produce higher hydrocarbons at 573 K. At the beginning of the experiment ethene and methane conversions were high (80–90% and 17–18%, respectively), but at the end, the selectivity shifted toward higher hydrocarbons. The product distribution varied in the absence of methane, suggesting that the presence of methane exerted a profound effect on the catalytic behavior. It was concluded that the catalysts interacted very strongly with methane, and a direct methane–ethene coupling was proposed in order to explain the formation of chain-lengthening products [187].

Ovalles et al. [188] studied the reaction of propene with methane using Ni/SiO_2, Ni/Al_2O_3 (see Table 12). They concluded that:

1. Ni/SiO_2 system was more active in the chain-lengthening reaction (81.4% selectivity to butanes) than Ni/Al_2O_3 catalyst (6.2% selectivity to C_4 compounds).
2. The metal dispersion of the Ni/SiO_2 catalyst was 100 times higher than that found for the Ni/Al_2O_3. In the latter case, metal was in the form of nickel aluminate ($NiAl_2O_4$).
3. The mechanism proposed involving the reaction of methane with the metal to generate CH_x species (x = 0, 1, 2, or 3), which in turn reacted with propene to produce butanes.

TABLE 12

Homologation of Propene [188]

Catalyst	Reaction	C_4 selectivity, %
Ni/Al_2O_3	$CH_4 + C_3H_6$	6.2
Ni/Al_2O_3	$N_2 + C_3H_6$	5.8
Ni/SiO_2[a]	$CH_4 + C_3H_6$	81.4
Ni/SiO_2	$N_2 + C_3H_6$	2.2
Ni/SiO_2[b]	$CH_4 + C_3H_6$	52.7
Ni/SiO_2	$H_2 + C_3H_6$	32.3

[a]Activated in a CH_4 flow of 10 cm^3/min at 873 K for 8 h.
[b]Activated in a CH_4 flow of 10 cm^3/min at 573 K for 8 h.

So far the action of the supported metals has been discussed. Methane also reacted with alkanes under oxidative conditions [189–191] in the presence of superacids [192,193] or Ziegler–Natta catalysts [194]. On aluminosilicates [195] and with various additives (e.g., dinitrogen oxide) [196], methane formed C_6 to C_{12} aromatic hydrocarbons. Alkanes were dimerized at 298 K on a silver-loaded zeolite by UV light [197]. Electron beam irradiation of a CH_4/CO_2 mixture results in the formation of hydrocarbons and hydrogen [198].

The underlying results clearly indicated that reactivity of the chemisorbed methane molecule depends on the nature of metals and on the morphology of transition metal. At strong methane adsorption the surface C_1 species are strongly bonded to the surface; thus they are only "spectator" species. On the other hand, supported metals such as nickel on various oxides are responsible for the formation of more reactive species. It is still to be decided whether this is due to the different surface structure of carbon or simply that the degree of methane dissociation is lower than on unsupported metals.

XI. PROMOTER EFFECT

The amount of literature on the effect of promoters is not too substantial. We demonstrated previously that carbidic carbon was not too reactive toward methane coupling because it was easily converted into graphitic carbon which is strongly bonded to the surface. Methane dissociation, which leads to CH_x species, required either small particles or large particles covered by patches of oxide promoter. Some of the data available are summarized here with the remark that it is a promising area to explore. Here we have to mention that the zeolite-supported metal catalysts, where small particles are present and are affected by the oxide environment, are the best candidates for this purpose.

The influence of vanadium promotion (oxophilic promoters) on the reactivity of adsorbed C atoms toward hydrogenation and C–C coupling has been investigated on rhodium-based catalysts [199,200]. The hydrogenation activity of the deposited carbon species on the rhodium catalyst was found to be 7 times higher than on the vanadium-promoted catalyst. The activation energy for this reaction appears to be about 7 kcal mol^{-1}. Hydrogenation at 473 K showed that reactivity of the carbon species toward higher hydrocarbons was increased by the vanadium promoter. This increased reactivity could not be due to a higher concentration of carbon species because the initial concentration of α-carbon was the same on both Rh and Rh/V catalysts. The increased reactivity must, therefore, be due to a changed intrinsic reactivity of the CH_x species. The chance for coupling of carbon fragments with respect to hydrogenation was five times higher on the vanadium-promoted catalyst. From the hydrogenation studies it appeared that vanadium suppressed the

reactivity of the absorbed carbon atoms. This agreed with the results on Ru carried out by Mori et al. [201], who investigated the rate of methanation of a pulse of CO in which k_{CO} and k_{CHx} could be separately measured. The ratio of k_{CHx}/k_{CO} for a Ru/Al_2O_3 catalyst was reduced by vanadium and molybdenum promotion.

The difficult step during hydrogenation of adsorbed carbon atoms on metal particles was related to the bond strength of the adsorbed CH_x intermediates. Slower hydrogenation was, therefore, probably due to a greater interaction between the carbon fragments and the metal surface. On the other hand, Meriadeau et al. [202] suggested that C–C bond formation was stimulated by more mobile CH_x fragments on rhodium catalysts, which was enhanced by TiO_2 promotion.

More recently, Chen et al. [203,207] studied the promoting effects of thoria and molybdena on Co/silica (alumina) catalysts on the hydrogenation of surface carbon fragments using temperature-programmed reduction (TPR) and temperature-programmed surface reduction (TPSR) techniques. TPR reduction profiles of the thoria/molybdena-promoted 10% Co/SiO_2 and Co/Al_2O_3 catalysts showed that the major consumption of hydrogen occurred at 573 and 633 K, respectively. Thoria was not reduced under these conditions; hence the consumption of hydrogen was due to the reduction of cobalt oxide, Co_3O_4, and CoO. The ratio of the hydrogen consumption at lower temperature to that measured at higher temperature was 1/3. This ratio was consistent with the reduction of cobalt oxide in two stages [204,205]:

$$Co_3O_4 + H_2 \rightarrow 3CoO + H_2O$$

$$3CoO + 3H_2 \rightarrow 3Co + 3H_2O$$

In the case of thoria/molybdena-promoted Co/SiO_2, the second peak shifted to higher temperature with the added thoria/molybdena, indicating that thoria/molybdena tended to stabilize the cobalt oxide (CoO). Consumption of hydrogen as shown by the second peak increased with added molybdena, because of the reduction of cobalt oxide and molybdena.

In the case of thoria/molybdena-promoted Co/Al_2O_3, the consumption of hydrogen from 573 to 673 K increased with the addition of thoria/molybdena, but the consumption near 973 K decreased. This behavior indicated that the promoter (thoria < molybdena) interacted more strongly with alumina than cobalt oxide and even spread onto the support beneath cobalt oxide. Thus thoria/molybdena shielded and weakened the interaction between cobalt oxide and the support.

In the temperature-programmed surface reaction, TPSR, the profiles demonstrated that on thoria/molybdena-promoted Co/SiO_2 catalysts, most methane was formed in a single peak. The temperature of the maximum decreased from 436 to 408 K and the amount of methane increased as the amount of added thoria/molybdena increased from 0% to 20% (10% in the case of molybdena). Thoria may enhance the dissociation of CO and facilitate

the formation of methane. When the added amount exceeded 20%, some thoria segregated and shielded the cobalt sites.

The TPSR profiles of the thoria/molybdena-promoted Co/Al_2O_3 catalysts show that methane is formed at two temperatures—at 426 K (methane formed from CO) and at 473 K (methane formed from methoxy complex adsorbed on alumina). Under the programmed condition, some adsorbed CO and H on cobalt spilled over to the alumina and associated to form methoxy complex (CH_3CO) [179,207]. The methoxy complex dissociated at a higher temperature and the CO diffused back and reacted with hydrogen to form methane on cobalt. The temperature of the first maximum decreased from 420 to 411 K as the amount of added thoria/molybdena increased from 0% to 20%. Thoria might promote dissociation of the CO adsorbed on cobalt. Molybdena was more effective at inhibiting the formation of methane from methoxy complex than thoria. These results indicated that molybdena/thoria (amount <15%) exhibited a greater tendency to spread onto alumina and impeded the spillover of CO and H from cobalt.

Hydrogenation of CO at 483 K and 1 bar over the thoria- and molybdena-promoted Co/SiO_2 catalysts showed that the activity enhanced (4 times in case of Th and 2.7 times in case of Mo) compared to that of the unpromoted one. Thoria (only active in the case of molybdena) promoted both the activity and the selectivity pattern, enhancing significantly the formation of olefins and long-chain hydrocarbons. Furthermore, added thoria resulted in increased activation energy. However, thoria and molybdena shielded the active sites and hampered the activity as the added amount exceeded 20% for thoria and 7% for molybdena.

The addition of thoria to 10% Co/Al_2O_3 catalyst also significantly increased the activity (molybdena slightly promoted the activity) by as much as 2.7 times that of the unpromoted one. The interaction between promoter and support weakened the effect of promoter on cobalt.

XII. EFFECT OF ALLOYS

The things which we have mentioned in the previous section also apply here. Modification of a metal by allowing it with an other metal may cause a synergism or simply a change in the activation mechanism and/or hydrogenation rate. This is again an area which must be pioneered in the future.

The catalytic effect of Ni–Cu alloys in many reactions has been the subject of a number of publications, including two reviews [208–210]. Recently, Bernardo et al. [211] studied steam reforming and decomposition of methane on silica-supported Ni–Cu catalysts to evaluate whether copper addition depresses the formation of carbon without affecting the main reaction. It was found that, in the absence of steam, the carbon deposition rate depended both vaguely (below 10 at.% Cu) and significantly (above 10at.% Cu) on the cooper content. At very high copper concentrations (80 at.%), a new

carbon structure was observed in which various filaments of nearly amorphous carbon were attached to the same metallic particle. This "octopus" carbon could not be observed at lower copper concentrations, in which the usual "whisker" structure, consisting of filaments with a metallic particle at the top, predominated [212]. For these concentrations, the carbon formation/gasification equilibrium in CH_4/H_2 mixtures was the same for the Ni–Cu alloys as for pure nickel catalysts.

In order to evaluate the effect of the catalyst composition on the nature of the carbon deposits formed on it, and the reactivity of the latter toward hydrogen, a series of temperature-programmed reactions (TPR) were performed by Tavares et al. [213], and they concluded that "octopus" carbon might be present in all deposits formed on Ni–Cu/SiO_2 catalysts with more than 10 at.% Cu in the metallic phase, together with "whisker" carbon, that is, on the catalysts for which the metal particle surfaces were strongly enriched in copper [211], and this predominated at 80 at.% Cu. This might be related to the change from a Type I to a Type II reaction, according to the classification of Ponec [209], observed in the deposition from methane above 10 at.% Cu [211].

The major drawback is the separation of the alloy particles [210] above 973 K in hydrocarbon, for example, in presence of ethylene. The deactivation phenomenon was extremely complex and involved not only the reaction, but also modification of the particles.

The mechanism and kinetics of formation of carbonaceous deposits from methane, *n*-hexane, 1,5-hexadiene, and benzene in the temperature range of 573–773 K on 1 wt% (Pt + xSn)/Al_2O_3 (x = 0.15, 0.3, 0.6, 1.2, 2 wt%) have been investigated [214]. Temperature-programmed oxidation (TPO) measurements revealed the formation of three types of carbonaceous deposits on the surface: DP-1 (may be precursor of coke), DP-2 (less reactive species), and DP-3 (highly unreactive species). Chemisorption and IR investigations have confirmed that DP-2 might be formed either by the "carbon" or by the "polyene" route. Apparently the presence of tin inhibited the formation of deposits via the "carbon" route but promoted the formation of deposits via the "polyene" route.

XIII. FURTHER WORKS

These experiments were carried out on silica-supported Ru, Co, and Rh [126–128] as well as on Pt, Pd, and Rh [59,134]. The key problem is how to stabilize the C_1 species and how to stabilize the catalysts. This includes the promotion of the formation of carbonaceous species, possibly in hydrogen-containing form, and hindering its surface transformation to nonreactive graphitic phase. Two alternatives can be predicted:

1. Modification of the support, including acid–base properties (e.g., zeolites)

2. Modification of the metal itself

Regarding the former case, a paper was recently published on Pt-loaded zeolite catalysts (Pt/HY and Pt/HX) [138] which were used in two-step methane conversion. A series of higher hydrocarbons were formed (ethane; propane; *n*- and *i*-butane; *n*-, cyclo-, and *i*-pentane; and a series of hexane isomers). On Pt/HX the conversion between 520 and 600 K did not change noticeably, whereas on Pt/HY there was decrease in the yield of higher hydrocarbons. Pt/HX was more active than Pt/HY above 520 K, which is just partly due to higher methane adsorption capacity.

Despite the cracking and isomerization activity of Pt, it may be suggested that here the acid–base properties of zeolite play important role in the high efficiency of methane conversion. Therefore, study could be recommended of the effects of acid properties of the support and promoters on this reaction. Using for example, $Pt/Nb_2O_5/Al_2O_3$ [215], two effects can be anticipated: first, after reduction Nb_2O_5 is reduced to NbO_x which decorate the surface of Pt depending on the niobia loading. Moreover, niobia becomes acidic, which apparently helps C_{2+} formation.

The metal part plays an important role. First, the property of metals, which helps methane cracking to form C_1 species on the surface (Ru, Co, Ni), is also an active species in the hydrogenolysis of the higher hydrocarbons formed. For example, on Ni during the reaction of *n*-hexane and hydrogen, C_7-hydrocarbons are formed. It has been shown that the fragments resulting from propene or *n*-hexane form surface carbon species which are able to increase the carbon number [184,185].

Besides, without hydrogen the surface carbon is easily transformed into graphitic forms. So we have to keep the balance between the accumulation (formation minus transformation) of CH_x species (where x is around 1) and hydrogenolysis activity. One possible method would be synergism by combination of two metals (one in minute quantity). For example, addition of small amount of Pd to α-iron supported on silicagel, higher hydrocarbons (up to C_7-hydrocarbons) are formed, whereas on pure iron only low molecular weight olefins are formed [216]. Here we have to mention also the work of Iglesia et al. [217]. Addition of small amount of Ru to Co/TiO_2 or Co/SiO_2 increased the turnover rate of C_{5+}-hydrocarbon production, and the catalyst can be reactivated at the same temperature.

To sum up, modification of the catalyst system—support and bimetallic effect—may give a possibility for the optimum performance of this two-step reaction. The temperature gap which exists between the two reactions may be narrowed by changing the parameters mentioned.

XIV. SUMMARY AND RECOMMENDATIONS

Low-temperature methane coupling, including the two-step process, partial oxidation, and homogeneous activation, has limitations. Processes like the

partial oxidation to CO + H_2 mixture have the drawback of the danger of large amount of CO_2 formation; the direct oxidation to oxygenates (methanol, formaldehyde) takes place with very low efficiency. At present the two-step process does not seem feasible because of the very low conversion, but improvements can be anticipated by:

- Lowering the temperature gap between the two reaction steps (carbon formation and hydrogenation)
- Stabilizing the catalyst activity
- Increasing the selectivity of (α-carbon) surface carbonaceous intermediate formation

The temperature gap may be narrowed by changing the following parameters:

- By increasing the methane pressure during adsorption
- By increasing the hydrogen pressure during hydrogenation

Stability of the catalyst and the CH_x species on the metal surface may be achieved by using bimetallic systems or promoters which "soften" the carbon–metal bond strength.

ACKNOWLEDGMENTS

The authors are indebted to the European Community Human Mobility Programme and the COST Programme (D5/01/93) for financial support.

REFERENCES

1. K. Fujimoto, *Stud. Surf. Sci. Catal.*, Vol. 81 (H. E. Curry-Hyde and R. F. Howe eds.), Elsevier, Amsterdam, 1994, p. 73.
2. J. R. Rostrup-Nielsen, *Catal. Today*, *21*, 257 (1994).
3. M. Baerns, K. van der Wiele, and J. R. H. Ross, *Catal. Today*, *4*, 471 (1989).
4. I. Pasquon, Plenary lecture at EUROPACAT-1, Montpellier, France, September 12–17, 1993.
5. J. H. Lunsford, *Stud. Surf. Sci. Catal.*, Vol. 61 (A. Holmen, K-I. Jens, and S. Kolboe, eds.), Elsevier, Amsterdam, 1991, p. 3; *Proc. 10th Int. Congress on Catal.* (L. Guczi, F. Solymosi, and P. Tétényi, eds.), Akadémiai Kiadó, Budapest, 1993, Vol. A, p. 103; *Stud. Surf. Sci. Catal.*, Vol. 81 (H. E. Curry-Hyde and R. F. Howe, eds.), Elsevier, Amsterdam, 1994, p. 1.
6. J. L. G. Fierro, *Catal. Lett.*, *22*, 67 (1993).
7. J. R. Rostrup-Nielsen, in *Catalysis, Science and Technology* (J. R. Anderson and M. Boudart, eds.), Vol. 5, Springer-Verlag, Berlin, 1984.
8. M. A. Vannice, *Catal. Rev.—Sci. Eng.*, *14*, 153 (1976).
9. H. Pichler, *Adv. Catal.*, *4*, 271 (1952).
10. C. D. Chang, *Stud. Surf. Sci. Catal.*, Vol. 61 (A. Holmen, K-I. Jens, and S. Kolboe, eds.), Elsevier, Amsterdam, 1991, p. 393.

11. S. T. Sie, M. M. G. Senden, and H. M. H. Wechem, *Catal. Today*, *8*, 371 (1991).
12. G. P. van der Zwet, P. A. J. M. Hendriks, and R. A. van Santen, *Catal. Today*, *4*, 365 (1989).
13. J. W. M. H. Geerts, Ph.D. Thesis, Eindhoven, 1990, p. 35.
14. G. E. Keller and M. M. Bhasin, *J. Catal.*, *73*, 9 (1982).
15. T. Ito, J-X. Wang, C. H. Lin, and J. H. Lunsford, *J. Am. Chem. Soc.*, *107*, 5062 (1985).
16. J. A. Sofranko, J. J. Leonard, and C. A. Jones, *J. Catal.*, *103*, 302 (1987).
17. K. Otsuka, K. Jinno, and A. Morikava, *Chem. Lett.*, 1985, p. 499.
18. A. T. Ashcroft, A. K. Cheetham, J. S. Ford, M. L. G. Green, C. P. Grey, A. J. Murrell, and P. D. F. Vernon, *Nature*, *334*, 319 (1990).
19. R. Pitchai and K. Klier, *Catal. Rev.*, *28*, 13 (1986).
20. H. Heinemann, G. A. Somorjai, P. Pereira, and S. H. Lee, *Catal. Lett.*, *6*, 266 (1990).
21. J. A. Roos, A. G. Bakker, H. Bosch, J. G. van-Ommen, and J. R. H. Ross, *Catal. Today*, *1*, 133 (1988).
22. Y. Jiang, I. V. Yentekakis, and C. G. Vayenas, *Science*, *264*, 1563 (1994).
23. T. Sundset, J. Sogge, and R. Porcelly, *Stud. Surf. Sci. Catal.*, Vol. 81 (H. E. Curry-Hyde and R. F. Howe, eds.), Elsevier, Amsterdam, 1994, p. 561.
24. G. D. Moggridge, T. Rayment, and R. M. Lambert, *J. Catal.*, *134*, 242 (1992).
25. K. Nomura, T. Hayakawa, K. Takehira, and J. Ujihira, *Appl. Catal. A*, *101*, 63 (1993).
26. Methane Activation (M. Baerns, J. R. H. Ross, and K. van der Wiele, eds.), *Catal. Today*, *4*, (1989); *Catal. Today*, *6*, (1990); C_1 Conversion: New Technology (G. J. Hutchings and M. S. Scurrell, eds.), *Catal. Today*, *8*, (1991); Catalytic Methane Conversion (C. Mirodatos, J. M. Basset, G. A. Martin, and J. Saint-Just, eds.), *Catal. Today*, *13* (1992); Catalytic Reactions of Partial Methane Oxidation (O. V. Krylov, ed.), *Catal. Today*, *18* (1993); Methane Activation (G. B. Marin, M. Baerns, M. Frias, and J. R. H. Ross, eds.), *Catal. Today*, *21* (1994); Recent Advance in C_1 Chemistry (G. J. Hutchings and M. S. Scurrell, eds.), *Catal. Today*, *23* (1995).
27. H. Mimoun, *N. J. Chem.*, *11*, 513 (1987).
28. A. Kiennemann, *Pet. Tech.*, *29*, 355 (1990).
29. T. Koerts and R. A. van Santen, *J. Mol. Catal.*, *70*, 119 (1991); ibid, *74*, 185 (1992); A. de Koster and R. A. van Santen, *J. Catal.*, *127*, 141 (1991).
30. H. Yang and J. L. Whitten, *Surf. Sci.*, *255*, 193 (1991).
31. A. B. Anderson, *J. Chem. Phys.*, *62*, 1187 (1975); A. B. Anderson, R. W. Grimes, and S. Y. Hong, *J. Chem. Phys.*, *91*, 4245 (1987).
32. P. J. Feibelman, *Phys. Rev. B.*, *26*, 5347 (1982).
33. M. A. Vannice, *J. Catal.*, *37*, 462 (1975).
34. R. A. van Santen, *Catal. Lett.*, *16*, 59 (1992).
35. R. W. Joyner, *Catal. Lett.*, *1*, 307 (1988).
36. E. Shustorovich, *Catal. Lett.*, *7*, 107 (1990).
37. C. Zheng, Y. Apeloig, and R. Hoffman, *J. Am. Chem. Soc.*, *110*, 749 (1988).
38. J. D. Beckerle, Q. Y. Yang, A. D. Johnson, and S. T. Ceyer, *J. Chem. Phys.*, *86*, 7236 (1987).

39. M. Kiskinova, in *New Trends in CO Activation* (L. Guczi, ed.), as in *Stud. Surf. Sci. Catal.*, Elsevier, Amsterdam, 1991, Vol. 64, p. 37.
40. E. G. M. Kuijpers, J. W. Jansen, A. J. van Dillen, J. W. Geus, *J. Catal.*, *72*, 75 (1981).
41. E. G. M. Kuijpers A. K. Breedijk, W. J. J. van der Wal, and J. W. Geus, *J. Catal.*, *72*, 210 (1981).
42. E. G. M. Kuijpers, A. K. Breedijk, W. J. J. van der Wal, and J. W. Geus, *J. Catal.*, *81*, 429 (1983).
43. J. Ekelens and W. J. Wosten, *J. Catal.*, *54*, 143 (1978).
44. N. A. Gajdaj, L. Babernics, and L. Guczi, *Kinet. Catal.*, *15*, 974 (1974) (in Russian).
45. O. Swang, K. Faegri, Jr., O. Gropen, and U. Wahlringen, *Stud. Surf. Sci. Catal.*, Vol. 61 (A. Holmen, K.-J. Jens, and S. Kolboe, eds.), Elsevier, Amsterdam, 1991, p. 191.
46. T. M. Duncan, P. Winslow, and A. T. Bell, *Chem. Phys. Lett.*, *102*, 163 (1983); *J. Catal.*, *95*, 305 (1985).
47. T. M. Duncan, P. Winslow, and A. T. Bell, *J. Catal.*, *93*, 1 (1985).
48. D. W. Goodman, R. D. Kelley, T. E. Madey, and Y. T. Yates, Jr., *J. Catal.*, *63*, 226 (1980).
49. J. W. Niemantsverdriet and A. D. van Langeveld, *Catalysis*, *89*, 769 (1987).
50. P. Winslow and A. T. Bell, *J. Catal.*, *86*, 158 (1984).
51. T. Mori, A. Miyamoto, N. Takahashi, M. Fukagaya, T. Hattori, and Y. Murakami, *J. Phys. Chem.*, *90*, 5197 (1986).
52. M. Araki and V. Ponec, *J. Catal.*, *44*, 439 (1976).
53. P. Biloen and W. M. H. Sachtler, *Adv. Catal.*, *30*, 165 (1981).
54. P. Winslow and A. T. Bell, *J. Catal.*, *94*, 385 (1985).
55. D. J. Trevor, D. M. Cox, and A. Kaldor, *J. Am. Chem. Soc.*, *112*, 3742 (1990).
56. A. D. van Langeveld, F. C. M. J. M. van Delft, and V. Ponec, *Surf. Sci.*, *135*, 93 (1983).
57. W. Kosowski and R. Dus, *Surf. Sci.*, *118*, 208 (1982).
58. S. G. Brass and G. Ehrlich, *Surf. Sci.*, *191*, L819 (1987).
59. F. Solymosi, A. Erdöhelyi, and J. Cserényi, *Catal. Lett.*, *16*, 399 (1992).
60. F. Solymosi, Gy. Kutsán, and A. Erdöhelyi, *Catal. Lett.*, *11*, 149 (1991).
61. F. Solymosi et al., *J. Catal.*, *141*, 287 (1993).
62. B. N. Shelimov and V. M. Kazansky, *J. C. S. Faraday Trans. I.*, *83*, 2381 (1978).
63. M. P. Kaminsky, N. Winograd, G. L. Geoffroy, and M. A. Vannice, *J. Am. Chem. Soc.*, *108*, 1315 (1986).
64. F. C. Schouten, O. L. J. Gijzeman, and G. A. Bootsma, *Surf. Sci.*, *87*, 1 (1979).
65. F. C. Schouten, E. W. Kaleveld, and G. A. Bootsma, *Surf. Sci.*, *63*, 460 (1977).
66. T. P. Beebe, Jr., D. W. Goodman, B. D. Kay, and J. T. Yates, Jr., *J. Chem. Phys.*, *87*, 2305 (1987).
67. J. T. Yates, Jr., S. M. Gates, and J. N. Russell, Jr., *Surf. Sci.*, *164*, L839 (1985).
68. Q. Y. Yang, A. D. Johnson, K. J. Maynard, and S. T. Ceyer, *J. Am. Chem. Soc.*, *11*, 8748 (1989).
69. H. He, J. Nakamura, and K. Tanaka, *Catal. Lett.*, *16*, 407 (1992).
70. M. B. Lee, Q. Y. Yang, and S. T. Ceyer, *J. Chem. Phys.*, *87*, 2724 (1987).

71. S. T. Ceyer, J. D. Beckerle, M. B. Lee, S. L. Tang, Q. Y. Yang and M. A. Hines, *J. Vac. Sci. Technol., A5*, 501 (1987).
72. S. T. Ceyer, *Langmuir, 6*, 82 (1990).
73. A. V. Hamza and R. J. Madix, *Surf. Sci., 179*, 25 (1987).
74. A. Morgante, S. Modesti, M. Bertolo, P. Rudolf, and R. Rosei, *Surf. Sci., 211/212*, 829 (1989).
75. P. Rudolf, C. Astaldi, S. Modesti, and R. Rosei, *Surf. Sci., 220*, L714 (1989).
76. P. H. McBreen, W. Erley, and H. Ibach, *Surf. Sci., 148*, 292 (1984).
77. Y. Zhou, M. A. Henderson, W. M. Feng, and J. M. White, *Surf. Sci., 224*, 386 (1989).
78. J. E. Parmeter, M. M. Hills, and W. H. Weinberg, *J. Am. Chem. Soc., 108*, 3563 (1986).
79. M.-C. Wo and D. W. Goodman, to be published.
80. P. Lenz-Solomun, M-C. Wo, and D. W. Goodman, *Catal. Lett., 25*, 75 (1994).
81. M.-C. Wo, D. W. Goodman, and G. W. Zajac, *Catal. Lett., 24*, 23 (1994).
82. F. Steinbach, J. Kiss, and R. Krall, *Surf. Sci., 157*, 401 (1985).
83. G. R. Schoots, C. R. Arumainayagam, M. C. McMaster, and R. J. Madix, *Surf. Sci., 215*, 1 (1989).
84. M. A. Henderson, G. E. Mitchell, and J. M. White, *Surf. Sci., 184*, L325 (1987).
85. Y. Zhou, W. M. Feng, M. A. Henderson, B. Roop, and J. M. White, *J. Am. Chem. Soc., 110*, 4447 (1988).
86. S. A. Costello, B. Roop, Z. M. Liu, and J. M. White, *J. Phys. Chem., 92*, 1019 (1988).
87. X. L. Zhou and J. M. White, *Chem. Phys. Lett., 142*, 376 (1987).
88. F. Solymosi, I. Kovács, and K. Révész, *Catal. Lett., 27*, 53 (1994).
89. F. Zaera, *Langmuir, 7*, 1998 (1991).
90. H. D. Gesser and L. A. Morton, *Catal. Lett., 11*, 357 (1991).
91. V. Ponec, in New Trends in CO Activation (L. Guczi, ed.), as in *Stud. Surf. Sci. Catal.*, Elsevier, Amsterdam, 1991, Vol. 64, p. 117.
92. P. R. Wentrcek, B. J. Wood, and H. Wise, *J. Catal., 43*, 363 (1976).
93. J. G. McCarty and H. Wise, *J. Catal., 57*, 406 (1979).
94. P. Biloen, J. N. Helle, and W. M. H. Sachtler, *J. Catal., 58*, 95 (1979); P. Biloen, *Recl. Trav. Chim. Pays-Bas, 99*, 33 (1980).
95. A. Takeuchi and J. R. Katzer, *J. Catal., 82*, 351 (1983).
96. T. Mori, A. Miyamoto, N. Takahashi, H. Niizuma, H. Hattori, and Y. Murakami, *J. Catal., 102*, 199 (1986).
97. A. T. Bell, *Proc. 9th Int. Congr. Catal.* (M. J. Phillips and M. Ternan, eds.), Chemical Institute of Canada, Ottawa, 1989, Vol. 5, p. 134.
98. P. Winslow and A. T. Bell, *J. Catal., 91*, 142 (1985).
99. H. Orita, S. Naito, and K. Tamaru, *J. Catal., 111*, 464 (1988).
100. D. G. Castner, R. L. Blackadar, and G. A. Somorjai, *J. Catal., 66*, 257 (1980).
101. V. Ponec, *Adv. Catal., 32*, 149 (1983).
102. K. Lázár, Z. Schay, and L. Guczi, *J. Mol. Catal., 17*, 205 (1982).
103. F. Fischer and M. Tropsch, *Brennst. Chem., 7*, 97 (1926); *Chem. Ber., 59*, 830 (1926).
104. S. R. Craxford and E. K. Rideal, *J. C. S. Chem. Commun.*, 1939, p. 1604.

105. A. Ekstrom and J. Lapszewicz, *J. Phys. Chem.*, *88*, 4577 (1984).
106. C. Ovalles, V. Leon, S. Reyes, and F. Rosa, *J. Catal.*, *129*, 368 (1991).
107. J. T. Kummer, Ph. H. Podgurski, W. B. Spencer, and P. H. Emmett, *J. Am. Chem. Soc.*, *73*, 564 (1951).
108. J. T. Kummer and P. H. Emmett, *J. Am. Chem. Soc.*, *75*, 5177 (1953).
109. L-M. Tau, H. Dabbagh, S. Bao, B. Chawla, J. Halász, and B. H. Davis, *Proc. 9th Int. Congr. Catal.* (M. J. Phillips and M. Ternan, eds.), Chemical Institute of Canada, Ottawa, 1988, Vol. 2, p. 861.
110. S. S. C. Chuang, Y. H. Tian, J. G. Goodwin, and I. Wender, *J. Catal.*, *96*, 396 (1985).
111. R. Nakamura, I. Takaahashi, C. S. Yong, and H. Niiyama, *Proc. 9th Int. Congr. Catal.* (M. J. Phillips and M. Ternan, eds.), Chemical Institute of Canada, Ottawa, 1988, Vol. 2, p. 759.
112. J. G. Ekerdt and A. T. Bell, *J. Catal.*, *62*, 19 (1980).
113. J. A. Baker and A. T. Bell, *J. Catal.*, *78*, 165 (1982).
114. R. C. Brady III and R. Petit, *J. Am. Chem. Soc.*, *102*, 6181 (1980); *103*, 287 (1981).
115. F. A. P. Cavalcanti, D. G. Blackmond, R. Oukaci, A. Sayari, A. Erdem-Senatalar, and I. Wender, *J. Catal.*, *113*, 1 (1988).
116. W. A. A. van Barneveld and V. Ponec, *J. Catal.*, *88*, 382 (1984).
117. F. A. P. Cavalcanti, R. Okaci, I. Wender, and D. G. Blackmond, *J. Catal.*, *128*, 311 (1991).
118. F. A. P. Cavalcanti, R. Oukaci, I. Wender, and D. G. Blackmond, *J. Catal.*, *123*, 260 (1990).
119. A. Deluzarche, J. P. Hindermann, A. Kiennemann, and R. Kieffer, *J. Mol. Catal.*, *31*, 225 (1985).
120. K. H. Theopold and R. G. Bergman, *J. Am. Chem. Soc.*, *103*, 2489 (1981).
121. K. Tanaka, I. Yaegashi, and K. Aomura, *J. C. S. Chem. Commun.*, 1982, p. 938.
122. S. Y. Hwang, E. G. Seebauer, and L. D. Schmidt, *Surf. Sci.*, *188*, 219 (1987).
123. S. Y. Hwang and L. D. Schmidt, *J. Catal.*, in press.
124. S. Y. Hwang, A. C. F. Kong, and L. D. Schmidt, *Surf. Sci.*, *217*, 179 (1989).
125. R. A. van Santen, A. de Koster, and T. Koerts, *Catal. Lett.*, *7*, 1 (1990).
126. T. Koerts and R. A. van Santen, *J. C. S. Chem. Commun.*, 1991, p. 1281.
127. T. Koerts, M. J. A. G. Deelen, and R. A. van Santen, *J. Catal.*, *138*, 101 (1992).
128. T. Koerts and R. A. van Santen, *J. Mol. Catal.*, *70*, 119 (1991).
129. R. A. van Santen, R. H. Cunningham, and J. H. B. J. Hoebink, *207th Nat. ACS Meeting*, *39*, 270 (1994).
130. T. Koerts, J. H. M. C. van Wolput, A. M. de Jong, J. W. Niemantsverdriet, and R. A. van Santen, *Appl. Catal. A*, *115*, 315 (1994).
131. N. Cheikhi, M. Ziyad, G. Coudurier, and J. C. Vedrine, *Appl. Catal. A*, *118*, 187 (1994).
132. F. Solymosi and J. Cserényi, *Catal. Today*, *21*, 561 (1994).
133. M. Belgued, P. Pareja, A. Amariglio, and H. Amariglio, *Nature*, *352*, 789 (1991).

134. M. Belgued, H. Amariglio, P. Pareja, A. Amariglio, and J. Saint-Just, *Catal. Today*, *13*, 437 (1992).
135. M. Belgued, S. Monteverdi, P. Pareja, H. Amariglio, A. Amariglio, and J. Saint-Just, Symposium on Natural Gas Upgrading, Div. Petr. Chem., ACS Meeting, San Francisco, April 5–10, 1992.
136. G. C. Bond and P. B. Wells, *Appl. Catal.*, *18*, 221 (1985).
137. P. Pareja, A. Amariglio, M. Belgued, and H. Amariglio, *Catal. Today*, *21*, 423 (1994).
138. E. Mielczarski, S. Monteverdi, A. Amariglio, and H. Amariglio, *Appl. Catal.*, *104*, 215 (1993).
139. C. Bezouhanova, J. Guidot, D. Barthomeuf, M. Breyse, and J. R. Bernard, *J. C. S. Faraday Trans. I*, *77*, 1581 (1981).
140. P. Gallezot, *Catal. Rev.—Sci. Eng.*, *20*, 121 (1979).
141. X. Bai and W. M. H. Sachtler, *Catal. Lett.*, *4*, 319 (1990).
142. A. P. J. Jansen and R. A. van Santen, in *Structure–Activity Relationship in Heterogeneous Catalysis* (R. K. Grasselli and A. W. Sleight, eds.), Elsevier, Amsterdam, 1991, p. 221.
143. V. B. Kazansky, V. Yu, Borovkov, N. Sokolova, N. I. Jaeger, and G. Schulz-Ekloff, *Catal. Lett.*, *23*, 263 (1994).
144. L. Wang, L. Tao, M. Xie, G. Xu, J. Huang, and Y. Xu, *Catal. Lett.*, *21*, 35 (1993).
145. F. Roessner and A. Hagen, *Stud. Surf. Sci. Catal.*, Vol. 81 (H. E. Curry-Hyde and R. F. Howe, eds.), Elsevier, Amsterdam, 1994, p. 569.
146. M. A. Long, S. J. X. He, M. I. Attalla, M. A. Wilson, and D. R. Smith, *Stud. Surf. Sci. Catal.*, Vol. 81 (H. E. Curry-Hyde and R. F. Howe, eds.), Elsevier, Amsterdam, 1994, p. 509.
147. V. D. Sokolovskii and S. S. Shepelev, *Stud. Surf. Sci. Catal.*, Vol. 81 (H. E. Curry-Hyde and R. F. Howe, eds.), Elsevier, Amsterdam, 1994, p. 497.
148. T. Nozaki and K. Fujimoto, *AIChE J.*, *40*, 870 (1994).
149. A. Andersen, I. M. Dahl, K.-J. Jens, E. Rytter, A. Slagtern, and A. Solbakken, *Catal. Today*, *4*, 389 (1989).
150. A. G. Anshits, A. N. Shigapov, S. N. Vereshshagin, and V. N. Shevnin, *Catal. Today*, *6*, 593 (1990).
151. C. Mirodatos, A. Holmen, R. Mariscal, and G. A. Martin, *Catal. Today*, *6*, 601 (1990).
152. C. Mirodatos, V. Ducarme, H. Mozzanega, A. Holmen, J. Sanchez-Marcano, Q. Wo, and G. A. Martin, *Stud. Surf. Sci. Catal.*, Vol. 61 (A. Holmen, K.-J. Jens, and S. Kolboe, eds.), Elsevier, Amsterdam, 1991, p. 41.
153. E. Iglesia and J. Baumgartner, *Catal. Lett.*, *21*, 55 (1993).
154. S. A. Driscoll, D. K. Gardner, and U. S. Ozkan, *Catal. Lett.*, *25*, 191 (1994).
155. L. Guczi, A. K. Sarma, Zs. Koppány, and A. Sárkány, paper submitted to 14th Meeting of the North American Catalysis Society, Snowbird, USA, June 10–16, 1995.
156. V. V. Eskova, A. E. Shilov, and A. A. Steinman, Kinet. *Catal.*, *13*, 534 (1982) (in Russian).
157. E. Gretz, T. F. Oliver, and A. Sen, *J. Am. Chem. Soc.*, *109*, 8109 (1987).
158. K. T. Nelson and K. Foger, *Stud. Surf. Sci. Catal.*, Vol. 81 (H. E. Curry-Hyde and R. F. Howe, eds.), Elsevier, Amsterdam, 1994, p. 545.

159. J. A. Labinger, J. E. Bercaw, G. A. Luinstra, D. K. Lyon, and A. M. Herring, *Stud. Surf. Sci. Catal.*, Vol. 81 (H. E. Curry-Hyde and R. F. Howe, eds.), Elsevier, Amsterdam, 1994, p. 515.
160. J. A. Labinger, A. M. Herring, and J. E. Bercaw, *J. Am. Chem. Soc.*, *112*, 5628 (1990).
161. K. Nakata, T. Miyata, Y. Yamaoka, T. Taniguchi, K. Takaki, and Y. Fujiwara, *Stud. Surf. Sci. Catal.*, Vol. 81 (H. E. Curry-Hyde and R. F. Howe, eds.), Elsevier, Amsterdam, 1994, p. 521.
162. D. Ekeberg, G. Hvistendahl, S. I. Hagen, C. Schulze, Y. Stenstrom, and E. Uggerud, *Stud. Surf. Sci. Catal.*, Vol. 61 (A. Holmen, K.-J. Jens, and S. Kolboe, eds.), Elsevier, Amsterdam, 1991, p. 201.
163. R. H. Crabtree, *Chem. Revs.*, *85*, 245 (1985).
164. M. J. Burk and R. H. Crabtree, *J. Am. Chem. Soc.*, *109*, 8025 (1987).
165. R. H. Crabtree, *Stud. Surf. Sci. Catal.*, Vol. 81 (H. E. Curry-Hyde and R. F. Howe, eds.), Elsevier, Amsterdam, 1994, p. 85.
166. R. A. Periana, D. J. Taube, E. R. Evitt, D. G. Löffler, P. R. Wentrcek, G. Voss, and T. Masuda, *Science*, *259*, 340 (1993).
167. R. A. Periana, D. J. Taube, E. R. Evitt, D. G. Löffler, P. L. Wentrcek, G. Voss, and T. Masuda, *Stud. Surf. Sci. Catal.*, Vol. 81 (H. E. Curry-Hyde and R. F. Howe, eds.), Elsevier, Amsterdam, 1994, p. 533.
168. S. Tenner, *Hydrocarbon Processing*, *66*, 52 (1987).
169. H. M. Swaan, V. C. H. Kroll, G. A. Martin, and C. Mirodatos, *Catal. Today*, *21*, 571 (1994).
170. J. Nakamura, K. Aikawa, K. Sato, and T. Uchijima, *Catal. Lett.*, *25*, 265 (1994).
171. K. Seshan, H. W. ten Barge, W. Hally, A. N. J. van Keulen, and J. R. H. Ross, *Stud. Surf. Sci. Catal.*, Vol. 81 (H. E. Curry-Hyde and R. F. Howe, eds.), Elsevier, Amsterdam, 1994, p. 285.
172. K. Fujimoto, K. Omata, T. Nozaki, and O. Yamazaki, Paper C42, 12th National Meeting of the North American Catalysis Society, Lexington, KY, May 1991.
173. J. H. Edwards, *Catal. Today*, *23*, 59 (1995).
174. I. D. Löffler, W. F. Maier, J. G. Andrade, I. Thies, and P. von Rague Schleyer, *J. Chem. Soc. Chem. Commun.*, 1984, p. 1177.
175. T. Koerts, P. A. Leclercq, and R. A. van Santen, *J. Am. Chem. Soc.*, *114*, 7272 (1992).
176. E. Rodriguez, M. Leconte, J.-M. Basset, K.-I. Tanaka, and K. Tanaka, *J. Am. Chem. Soc.*, *110*, 275 (1988).
177. M. S. Scurrell, *Appl. Catal.*, *32*, 1 (1987).
178. G. A. Oláh, J. D. Felberg, and K. Lammertsma, *J. Am. Chem. Soc.*, *105*, 6529 (1983).
179. T. Koerts and R. A. van Santen, *J. C. S. Chem. Commun.*, 1992, p. 345.
180. K. Tanaka and K.-I. Tanaka, *J. C. S. Chem. Commun.*, 1984, p. 1626.
181. K. Tanaka, K.-I. Tanaka, H. Takeo, and C. Matsumura, *J. C. S. Chem. Commun.*, 1986, p. 33.
182. L. Guczi, A. Sárkány, and P. Tétényi, Proc. 5th Int. Congr. Catal., North Holland, Amsterdam, 1973, Vol. 2, p. 1111.

183. L. Guczi, J. Kálmán, and A. Sárkány, in *Mechanism of Hydrocarbon Reactions* (D. Kalló and F. Márta, eds.), Akadémiai Kiadó, 1975, p. 175.
184. A. Sárkány, L. Guczi, and P. Tétényi, *React. Kinet. Catal. Lett., 1*, 169 (1974).
185. L. Guczi, J. Kálmán, and K. Matusek, *React. Kinet. Catal. Lett., 1*, 51 (1974).
186. P. R. J. Schleyer, I. D. Löffler, W. F. Mair, and J. G. Andrade, *J. C. S. Chem. Commun.*, 1984, p. 1178.
187. M. S. Scurrell, *Appl. Catal., 34*, 109 (1987).
188. C. Ovalles, V. Leon, S. Reyer, and F. Rosa, *J. Catal., 129*, 368 (1991).
189. J. Haggin, *Chem. Eng. News, 42*, 29 (1983).
190. G. E. Keller and M. M. Bhasin, *J. Catal., 73*, 9 (1982).
191. K. G. Ione, *Khim. Tver. Topl., 6*, 35 (1982).
192. J. Sommer, M. Muller, and K. Laali, *Nouv. J. Chim., 6*, 3 (1982).
193. G. A. Olah, Eur. Pat. Appl. EP 73673 (cl.CO7C2/76) March 9, 1983 (*Chem. Abs., 98*, 218647m, 1983).
194. N. F. Noskova, D. V. Sokolskii, M. B. Izteleuova, and N. A. Garafova, *Dokl. Akad. Nauk SSSR, 262*, 113 (1982) (*Chem. Abs., 96*, 142199c, 1982).
195. O. V. Bragin, T. V. Vasina, Ya. I. Isakov, B. K. Nefedov, A. V. Preobrazhenskii, N. V. Palishkina, and Kh. M. Minachev, *Izv. Akad. Nauk USSR, Ser. Khim.*, 1982, p. 954; O. V. Bragin, T. V. Vasina, Ya. I. Isakov, B. K. Nefedov, A. V. Preobrazhenskii, N. V. Palishkina, and Kh. M. Minachev, *Izv. Akad. Nauk USSR, Ser. Khim.*, 1982, p. 954.
196. D. Young, Eur. Pat. Appl. EP 93543 (Cl.CO7C15/00), November 9, 1983.
197. G. A. Ozin and F. Hugues, *J. Phys. Chem., 86*, 5174 (1982).
198. H. Arai, S. Nagai, and M. Hatada, *Z. Phys. Chem. N. F., 131*, 69 (1982).
199. T. Koerts and R. A. van Santen, *Catal. Lett., 6*, 49 (1990).
200. R. H. Cunningham, A. V. G. Mangnus, J. van Grondelle, and R. A. van Santen, *Catal. Today, 21*, 431 (1994).
201. T. Mori, A. Miyamoto, N. Takahash, M. Fukagaya, H. Niizuma, T. Hattori, and Y. Murakami, *J. C. S. Chem. Commun.*, 1984, p. 678.
202. P. Meriaudeau, J. F. Dutel, M. Dufaux, and C. Naccache, *Stud. Surf. Sci. Catal.*, Vol. 11 (B. Imelik, C. Naccache, G. Courdurier, H. Praliaud, P. Meriaudeau, P. Gallezot, G. A. Martin, and J. C. Vedrine, eds.), Elsevier, Amsterdam, 1982, p. 95.
203. Y. Z. Chen and T. H. Wang, *Catal., Lett., 22*, 165 (1993).
204. B. Viswanathan and R. Gopalakrishnan, *J. Catal., 99* 342 (1986).
205. P. Arnoldy and J. A. Moulijn, *J. Catal., 93*, 38 (1985).
206. W. H. Lee and C. H. Bartholomew, *J. Catal., 120*, 256 (1989).
207. P. G. Glugla, K. M. Bailey, and J. L. Falconer, *J. Phys. Chem., 92*, 4474 (1988), and *J. Catal., 115*, 24 (1989); B. Chen and J. L. Falconer, *Catal. Lett., 19*, 55 (1993).
208. K. C. Khulbe and R. S. Mann, *Catal. Rev.—Sci. Eng., 24*, 311 (1982).
209. V. Ponec, *Int. J. Quantum Chem., 12*, Suppl. 2, 1 (1977).
210. N. M. Rodriguez, M. S. Kim, and R. T. K. Baker, *J. Catal., 140*, 16 (1993).
211. C. A. Bernardo, I. Alstrup, and J. R. Rostrup-Nielsen, *J. Catal., 96*, 517 (1985).
212. R. T. K. Baker, M. A. Barber, P. S. Harris, F. S. Feates, and R. J. Waite, *J. Catal., 26*, 51 (1972).

213. M. T. Tavares, C. A. Bernardo, I. Alstrup, and J. R. Rostrup-Nielsen, *J. Catal.*, *100*, 545 (1986).
214. A. Sárkány, H. Lieske, T. Szilágyi, and L. Tóth, *Proc. 8th Int. Congr. Catal.*, Verlag Chemie, Weinheim, 1985, Vol. 2, p. 613.
215. T. Hoffer, Z. Zsoldos, and L. Guczi, *J. Mol. Catal.*, *92*, 167 (1994).
216. M. Nimz, G. Lietz, J. Völter, K. Lázár, and L. Guczi, *Catal. Lett.*, *1*, 93 (1988).
217. E. Iglesia, S. L. Soled, R. A. Fiato, and G. H. Via, *J. Catal.*, 143, 345 (1993).